MOLECULAR AND CELLULAR BIOLOGY, Aug. 2009, p. 4308–4324 Vol. 29, No. 15
0270-7306/09/$08.00+0 doi:10.1128/MCB.01665-08

Site-Specific mTOR Phosphorylation Promotes mTORC1-Mediated Signaling and Cell Growth▽

Hugo A. Acosta-Jaquez,[1] Jennifer A. Keller,[1] Kathryn G. Foster,[1] Bilgen Ekim,[1] Ghada A. Soliman,[1,2] Edward P. Feener,[4] Bryan A. Ballif,[3] and Diane C. Fingar[1,2]*

Department of Cell and Developmental Biology[1] and Department of Medicine, Division of Metabolism, Endocrinology, and Diabetes,[2] 109 Zina Pitcher Place, University of Michigan Medical School, Ann Arbor, Michigan 48109-2200; Joslin Diabetes Center, One Joslin Place, Boston, Massachusetts 02215[4]; and Department of Biology and Vermont Genetics Network Proteomics Facility, University of Vermont, 311 March Life Science Building, Burlington, Vermont 05405[3]

Received 27 October 2008/Returned for modification 15 December 2008/Accepted 22 May 2009

The mammalian target of rapamycin (mTOR) complex 1 (mTORC1) functions as a rapamycin-sensitive environmental sensor that promotes cellular biosynthetic processes in response to growth factors and nutrients. While diverse physiological stimuli modulate mTORC1 signaling, the direct biochemical mechanisms underlying mTORC1 regulation remain poorly defined. Indeed, while three mTOR phosphorylation sites have been reported, a functional role for site-specific mTOR phosphorylation has not been demonstrated. Here we identify a new site of mTOR phosphorylation (S1261) by tandem mass spectrometry and demonstrate that insulin–phosphatidylinositol 3-kinase signaling promotes mTOR S1261 phosphorylation in both mTORC1 and mTORC2. Here we focus on mTORC1 and show that TSC/Rheb signaling promotes mTOR S1261 phosphorylation in an amino acid-dependent, rapamycin-insensitive, and autophosphorylation-independent manner. Our data reveal a functional role for mTOR S1261 phosphorylation in mTORC1 action, as S1261 phosphorylation promotes mTORC1-mediated substrate phosphorylation (e.g., p70 ribosomal protein S6 kinase 1 [S6K1] and eukaryotic initiation factor 4E binding protein 1) and cell growth to increased cell size. Moreover, Rheb-driven mTOR S2481 autophosphorylation and S6K1 phosphorylation require S1261 phosphorylation. These data provide the first evidence that site-specific mTOR phosphorylation regulates mTORC1 function and suggest a model whereby insulin-stimulated mTOR S1261 phosphorylation promotes mTORC1 autokinase activity, substrate phosphorylation, and cell growth.

The mammalian target of rapamycin (mTOR), an evolutionarily conserved serine/threonine protein kinase, senses and integrates signals from diverse environmental cues (14, 31, 50, 74). mTOR associates with different partner proteins to form functionally distinct signaling complexes (4). The immunosuppressive drug rapamycin acutely inhibits signaling by mTOR complex 1 (mTORC1) (22), which contains mTOR, mLST8/GβL, raptor, and PRAS40 (24, 33, 34, 54, 67). Rapamycin fails to acutely inhibit signaling by mTORC2, which contains mTOR, mLST8/GβL, rictor, mSin1, and PRR5/Protor (18, 32, 47, 55, 73, 76). mTORC1 promotes various biosynthetic processes, including protein synthesis, cell growth (an increase in cell mass and size), and cell proliferation (an increase in cell number) (14, 40, 74). During growth factor (e.g., insulin) and nutrient (e.g., amino acids and glucose) sufficiency, mTORC1 phosphorylates the translational regulators p70 ribosomal protein S6 kinase 1 (S6K1) and eukaryotic initiation factor 4E binding protein 1 (4EBP1) to coordinately upregulate protein biosynthesis (40). Both S6K1 and 4EBP1 contain a TOR signaling motif, which mediates their interaction with raptor and thus facilitates their recruitment to the mTOR kinase (10, 44, 57, 58). In addition to regulating protein synthesis, mTORC1-mediated phosphorylation of S6K1 and 4EBP also promotes cell growth and cell cycle progression (15, 16). While more recently identified and thus less well characterized than mTORC1, mTORC2 mediates the phosphorylation of AGC kinase family members (e.g., Akt [also known as protein kinase B, PKB], PKCα, and SGK1) on their hydrophobic motifs and modulates the organization of the actin cytoskeleton (20, 26, 32, 55, 56).

The insulin pathway represents the best-characterized activator of mTORC1 signaling to date, and thus many signaling intermediates that link insulin receptor activation to mTORC1 have been identified (12, 31). Complementary work using *Drosophila melanogaster* genetics and mammalian cell culture identified TSC1 (hamartin) and TSC2 (tuberin) as upstream negative regulators of mTORC1 (27). Inactivation of either the *TSC1* or *TSC2* genes, whose protein products heterodimerize to form a tumor suppressor complex, causes the development of benign tumors in diverse organs in both humans and rodents, a disease known as tuberous sclerosis complex (TSC) (36). TSC2 contains a GTPase-activating protein domain that acts on Rheb, a Ras-like GTP binding protein that activates mTORC1 (27). Thus, in TSC-deficient cells, constitutive Rheb-GTP leads to chronically high mTORC1 signaling. While the mechanism by which Rheb-GTP activates mTORC1 remains incompletely understood, Rheb coimmunoprecipitates with mTOR and directly activates mTORC1 kinase activity in vivo and in vitro when GTP bound (2, 38, 54). Rheb has been reported to augment the activity of PLD1, an enzyme that catalyzes the production of the lipid second messenger phosphatidic acid, which contributes to the mitogenic activation of

* Corresponding author. Mailing address: Department of Cell and Developmental Biology, 109 Zina Pitcher Place, University of Michigan Medical School, Ann Arbor, MI 48109-2200. Phone: (734) 763-7541. Fax: (734) 763-1166. E-mail: dfingar@umich.edu.

▽ Published ahead of print on 1 June 2009.

mTORC1 signaling (13, 62). Additionally, Rheb-GTP was reported to induce the dissociation of the endogenous mTOR inhibitor FKBP38 (3), although aspects of this model have been questioned (72). Insulin/phosphatidylinositol 3-kinase (PI3K) signaling reduces the inhibitory effect of TSC on mTORC1 via Akt-mediated phosphorylation of TSC2 (29, 42, 64). Additionally, Ras-regulated signaling via mitogen-activated protein kinase (MAPK) and RSK also inhibits TSC via PI3K/Akt-independent phosphorylation of TSC2 (39, 51, 63). In contrast, glucose deprivation enhances TSC's inhibitory effect on mTORC1 signaling via AMP-activated protein kinase (AMPK)-mediated phosphorylation of TSC2 (on different sites) (30). Thus, TSC functions as a central nexus of diverse physiological signals to fine-tune mTORC1 signaling depending on environmental conditions (27). While the mechanism by which amino acids promote mTORC1 signaling has remained elusive, compelling new data reveal that the Rag GTPases link amino acid sensing to mTORC1 activation (35, 52, 53). During amino acid sufficiency, GTP-bound Rag heterodimers bind raptor and recruit mTORC1 to an endomembrane compartment that contains the mTORC1 activator Rheb; thus, amino acid sufficiency may function to prime mTORC1 for subsequent growth factor-mediated activation via a dynamic subcellular redistribution mechanism (52).

Despite the well-characterized regulation of mTORC1 signaling by growth factors (e.g., insulin), nutrients (e.g., amino acids and glucose), and cellular stress (e.g., hypoxia) and the identification of numerous signaling mediators of these pathways, the direct molecular mechanisms by which cellular signals modulate mTORC1 action remain obscure (31). While three phosphorylation sites (P-sites) on mTOR have been reported to date (T2446, S2448, and S2481), no function has yet been ascribed to any site (7, 43, 49, 59). Here we identify S1261 as a novel mTOR phosphorylation site in vivo in cultured mammalian cells and provide the first evidence that site-specific mTOR phosphorylation regulates mTORC1 function. We show that insulin signals via the PI3K/TSC/Rheb pathway in an amino acid-dependent and rapamycin-insensitive manner to promote mTOR S1261 phosphorylation, which regulates mTORC1 autokinase activity, biochemical signaling to downstream substrates, and cell growth to increased cell size, a major cellular function of mTORC1. Elucidation of the molecular mechanisms underlying mTORC1 regulation will enable us to better understand how mTORC1 senses environmental stimuli to control cellular physiology. As aberrantly upregulated mTORC1 signaling likely contributes to cancer, insulin-resistant diabetes, and cardiovascular diseases, understanding mTORC1 regulation may aid in the development of novel therapeutics for these prevalent human diseases (11, 21, 28).

MATERIALS AND METHODS

Materials. Reagents were obtained from the following sources: protein A-Sepharose CL4B and protein G-Sepharose Fast Flow were from GE Healthcare; 3-[(3-cholamidopropyl)-dimethylammonio]-1-propanesulfonate (CHAPS) was from Pierce; Immobilon-P polyvinylidene difluoride (PVDF) membrane (0.45 μm) was from Millipore; autoradiography film (HyBlot CL) was from Denville Scientific; reagents for enhanced chemiluminescence (ECL) were from Millipore (Immobilon Western chemiluminescent horseradish peroxidase [HRP] substrate); all chemicals were from either Fisher Chemicals or Sigma.

Commercial antibodies. AU1, Myc (9E10), and HA (HA.11) antibodies were from Covance. Flag-M2 antibody was from Sigma, and Rheb antibody was from AbCam. Donkey anti-rabbit antibody–HRP and sheep anti-mouse antibody–HRP were from GE Healthcare. The following antibodies were from Cell Signaling Technology: P-S6K1 (Thr389; rabbit monoclonal 108D2), S6, mTOR P-S2481, P-Akt (S473), total Akt, P-4EBP1 (T37/46), P-4EBP1 (S65), P-4EBP1 (T70), and total 4EBP1. Tubulin monoclonal antibody was a gift from K. Verhey (University of Michigan Medical School, Ann Arbor).

Custom generation of antibodies to raptor, mTOR, P-S1261-mTOR, rictor, S6K1, and P-S6. To generate immunogen, peptides, and P-peptides (70% pure; synthesized by Boston Biomolecules, Woburn, MA [now called Advanced Peptides, Inc., Boston, MA]) were coupled via an N-terminal cysteine to maleimide-activated mariculture keyhole limpet hemocyanin (mcKLH; Pierce). Antipeptide antibodies were affinity purified by positive selection on antigen peptide that was coupled to Affigel matrix (Bio-Rad). Phospho-peptide antibodies were affinity purified by positive selection on antigen phospho-peptide followed by negative selection on cognate antigen non-phospho-peptide and irrelevant phospho-peptide (either a P-Ser Jak2 or a P-Thr-Jak2 peptide). The following peptides were used to generate antibodies ("p" indicates a phosphorylated residue): (i) raptor (amino acids 885 to 901; human; CSSSLTNDVAKQPVSRDL); (ii) mTOR (amino acids 221 to 237; rat; CTQREPKEMQKPQWYRHT); (iii) P-S1261-mTOR [amino acids 1256 to 1266; rat; CKKLHV(pS)TINLQ]; (iv) rictor (amino acids 6 to 20; human; CRGRSLKNLRVRGRND); (v) S6K1 (C-terminal 17 amino acids 485 to 502 of the 70-kDa rat isoform; CKQAFPMISKRPEHLRM NL); (vi) P-S6 [amino acids 232 to 249; CRRL(pS)(pS)LRA(pS)TSK(pS)EE (pS)QK].

Plasmids. The pcDNA3/AU1-mTOR wild-type (WT), rapamycin-resistant (RR; S2035I), kinase-dead (KD; S2338A), and RR/KD (S2035I; D2338A) plasmids were generated by R. Abraham (Wyeth, Pearl River, NY); the pRK5/Myc-raptor plasmid was provided by D. Sabatini (MIT, Boston, MA); pRK5/Myc-mTOR and pRK5/Myc-mTOR-KD were obtained from D. Sabatini via Addgene (nos. 1861 and 8482, respectively); the pRK7/HA-S6K1, pKH3/HA-mLST8/GβL, and pRK7/Flag-Rheb plasmids were from J. Blenis (Harvard Medical School, Boston, MA), and pACTAG2/3HA-4EBP1 was from N. Sonenberg (McGill, Montreal, Canada).

Mass spectrometric analysis to identify mTOR P-sites. HEK293 cells (20 15-cm plates per condition; $\sim 15 \times 10^6$ cells/15-cm plate) were untransfected or transiently transfected with AU1-tagged mTOR (25 μg) and cultured in Dulbecco's modified Eagle's medium (DMEM) with 10% fetal bovine serum (FBS) or in growth factor and amino acid-stimulated medium (DMEM plus insulin; 30 min) after factor deprivation (via serum withdrawal for 24 h followed by incubation in Dulbecco's phosphate-buffered saline [D-PBS]–glucose for 60 min). AU1-mTOR was immunoprecipitated overnight, resolved by sodium dodecyl sulfate-polyacrylamide gel electrophoresis (SDS-PAGE), and stained with Coomassie blue R-250. AU1-mTOR protein was excised from the gel, digested with trypsin, and analyzed by tandem mass spectrometry.

In-gel digestion, mass spectrometry, and data analysis. Cubed Coomassie-stained gel bands of immunoprecipitated AU1-tagged rat mTOR were rinsed with water, destained with 50% acetonitrile (MeCN), 50% ammonium bicarbonate, dehydrated with 100% MeCN, and subjected to in-gel digestion with 6 ng/μl sequencing-grade modified trypsin (Promega) in 50 mM ammonium bicarbonate for 16 h at 37°C. Peptides were extracted once with 50% MeCN, 2.5% formic acid (FA), and once with 100% MeCN. Dried peptides were resuspended in 2.5% MeCN, 2.5% FA, and loaded using a Micro AS autosampler (Thermo Electron) and a Surveyor MS Pump Plus (Thermo Electron) onto a nano-electrospray microcapillary column packed with 14 cm of reverse-phase MagicC_{18} material (5 μm; 200Å; Michrom Bioresources, Inc.). Elution was performed with a 5 to 35% MeCN (0.15% FA) gradient over 45 min, after a 15-min isocratic loading at 2.5% MeCN, 0.15% FA. Solvent A was 2.5% MeCN, 0.15% FA, and solvent B was 99.85% MeCN, 0.15% FA. Mass spectra were acquired in an LTQ linear ion trap mass spectrometer (Thermo Electron). Throughout the entire run, 10 data-dependent tandem mass spectrometry (MS/MS) scans were acquired on the most abundant ions in dynamic exclusion mode following a precursor survey (MS1) scan. Mass spectral data were searched against a rat mTOR protein database using Turbo SEQUEST (Thermo Electron, version 27, revision 12) requiring no enzyme specificity and a 2-Da precursor mass tolerance. Cysteine residues were required to have a static increase of 71.0 Da for acrylamide (C_3H_5ON) adduction. Differential modification of 16.0 Da on methionine and 80.0 Da on serine, threonine, and tyrosine was permitted.

cDNA mutagenesis and sequencing. Site-directed mutagenesis was performed using QuikChange II XL (Stratagene), and cDNA inserts in mutated plasmids were fully sequenced. We generated the following mutations in WT and RR pcDNA3/AU1-mTOR backbones: S1261A, S1261D, and S2481A. We generated

the following mutations in pRK5/Myc-mTOR: RR (S2035I), S1261A, RR/S1261A, RR/S1261D, and S2481A. The following oligonucleotides were used to create point mutations in the rat mTOR cDNA (accession number L37085) (capital letters indicate mismatches, and the three underlined nucleotides represent the codon mutated): *S1261A*, primer 1, 5′-gaagaaactgcatgtcGCCaccatcaa cctcc-3′, and primer 2, 5′-ggaggttgatggtgGCGacatgcagtttcttc-3′; *S1261D*, primer 1, 5′-gaagaaactgcatgtcGACaccatcaacctcc-3′, and primer 2, 5′-ggaggttgatggtgTCGacatgcagtttcttc-3′; *S2481A*, primer 1, 5′-tgccagaatccatccatgcCttcattggagatggtttgg-3′, and primer 2, 5′-ccaaaccatctccaatgaaGGcatggatggattctggca-3′; *S2035I*, primer 1, 5′-ggcctagaagaggccATtcgcttgtactttggg-3′, and primer 2, 5′cccaaagtacaagcgaATggcctcttctaggcc-3′.

Generation of shRNA-encoding lentiviruses and lentiviral infection. shRNA-encoding lentiviruses were generated via the protocol posted on the Addgene website (http://www.addgene.org/pgvec1). Briefly, 7×10^5 HEK293T cells on 60-mm plates were cotransfected with pLKO.1 shRNA plasmid (1 μg), pCMV-dR8.2 dvpr (Addgene number 8455) packaging plasmid (750 ng), and pCMV-VSVG (Addgene number 8454) envelope plasmid (250 ng) using FuGENE transfection reagent. The next morning, the cells were refed with 5 ml fresh medium (DMEM–10% FBS). After 24 h, the virus-containing medium was harvested, and another 5 ml of fresh medium was added. After 24 h, the viral-containing medium was harvested a second time, pooled with the first collection, and filtered (0.45 μm). Viral infection was performed by adding 500 μl of virus-containing medium to a ~70% confluent plate of $TSC1^{-/-}$ mouse embryonic fibroblasts (MEFs) that were fed with fresh medium containing 8 μg/ml Polybrene. After 24 h, cells were split 1:10 (due to the high proliferation rate) and selected for ~6 days in fresh medium containing 2.5 μg/ml puromycin. The following plasmids were used: pLKO.1-scramble shRNA (Addgene number 1864), pLKO.1 Rheb-1 (Open Biosystems number TRCN0000075603), and pLKO.1 Rheb-3 (Open Biosystems number TRCN0000075605) (the Rheb shRNA plasmids were kindly shared by John Blenis, Harvard Medical School, Boston, MA). The hairpin sequence for the mouse-specific Rheb-1 shRNA was the following: 5′-CCGGCCCGTCATCCTTGAAGATAAACTCGAGTTTATC TTCAAGGATGACGGGTTTTTG-3′. The hairpin sequence for the mouse-specific Rheb-3 shRNA was the following: 5′-CCGGCAGACATACTCCATAG ATATTCTCGAGAATATCTATGGAGTATGTCTGTTTTTG-3′.

Cell culture, drug treatment, and transfection. HEK293 cells and immortalized $TSC1^{+/+}$ and $TSC1^{-/-}$ mouse embryonic fibroblasts (originally from D. Kwiatkowski, Brigham and Women's Hospital, Boston, MA) were cultured in DMEM that contained high glucose (4.5 g/liter), glutamine (584 mg/liter), and sodium pyruvate (110 mg/liter; Gibco/Invitrogen) supplemented with 10% FBS (HyClone). 3T3-L1 fibroblasts were differentiated into adipocytes by a standard protocol (41, 61). All cells were incubated at 37°C in a humidified atmosphere containing 5% CO_2. All cells were serum deprived via incubation in DMEM supplemented with 20 mM HEPES (pH 7.2) for ~20 h. Insulin (100 nM; Invitrogen) was added to serum-deprived cells for 30 min. For drug treatment, serum-deprived cells were pretreated with rapamycin (20 ng/ml; Calbiochem) or wortmannin (100 nM; Upstate/Millipore) for 30 min prior to the addition of insulin; cells proliferating in DMEM-FBS (steady state) were pretreated with drugs for 1 to 2 h. To effect amino acid deprivation, HEK293 cells were incubated in Dulbecco's PBS containing D-glucose (1 g/liter) and sodium pyruvate (36 mg/liter; D-PBS/Glc) for 60 min. HEK293 cells on 60-mm plates were transfected using TransIT-LT1 (Mirus) and a total of 4 to 5 μg of DNA per plate; the specific amounts of experimental plasmid transfected are stated in the figure legends. Cells were lysed ~24 to 48 h posttransfection.

Cell lysis, immunoprecipitation, and immunoblotting. Cells were washed twice with ice-cold PBS and scraped into ice-cold lysis buffer A (10 mM KPO_4, pH 7.2, 1 mM EDTA, 5 mM EGTA, 10 mM $MgCl_2$, 50 mM β-glycerophosphate, 1 mM sodium orthovanadate [Na_3VO_4], 5 μg/ml pepstatin A, 10 μg/ml leupeptin, 40 μg/ml phenylmethylsulfonyl fluoride [PMSF]) containing CHAPS (0.3%) (to preserve the mTOR-Raptor interaction postlysis) (24, 33) or NP-40 (0.5%) and Brij35 (0.1%). Lysates were spun at 13,200 rpm for 5 min at 4°C, and the postnuclear supernatants were collected. The Bradford assay was used to normalize protein levels for immunoprecipitation and immunoblot analyses. For immunoprecipitation, whole-cell lysates (WCL) were incubated with antibodies for ~2 h (overnight for AU1 immunoprecipitations) at 4°C, incubated with protein A- or G-Sepharose beads for 1.5 h, washed three times in lysis buffer, and resuspended in 1× sample buffer (50 mM Tris-HCl, pH 6.8, 10% glycerol, 2% SDS, 2% β-mercaptoethanol, 0.02% bromophenol blue). Samples were resolved on SDS-PAGE gels and transferred to PVDF membranes by using Towbin transfer buffer (25 mM Tris, 192 mM glycine, 10% methanol, 0.02% SDS). Immunoblotting was performed by blocking PVDF membranes in Tris-buffered saline with Tween 20 (TBST; 40 mM Tris-HCl, pH 7.5, 0.9% NaCl, 0.1% Tween 20) containing 3% nonfat milk and incubating the membranes in TBST with 2% bovine serum albumin containing primary antibodies or secondary HRP-conjugated antibodies. Blots were developed by ECL.

Treatment of mTOR with λ-phosphatase. Following mTOR immunoprecipitation, beads were washed three times in CHAPS lysis buffer followed by two additional washes in ST buffer (50 mM Tris-HCl, pH 7.2; 150 mM NaCl). Beads were then resuspended in 1× phosphatase buffer (50 mM Tris-HCl, pH 7.5, 100 mM NaCl, 2 mM dithiothreitol, 0.1 mM EGTA, 0.01% Brij 35) that contained 2 mM $MnCl_2$. Samples were incubated at 30°C for 30 min in the absence or presence of λ-phosphatase (Invitrogen), and reactions were terminated by adding EDTA, pH 8.0, to a 50 mM final concentration and sample buffer to a 1× final concentration. Six percent SDS-PAGE gels were run at 8 mA for ~16 h.

S6K1 in vitro kinase assays. Lysates from HA-S6K1 transfected cells were immunoprecipitated with anti-hemagglutinin (HA) antibodies for 2 h and incubated with protein G-Sepharose beads for 1.5 h. Immune complexes were each washed in 1 ml of ice-cold buffer A (10 mM Tris-HCl, pH 7.2, 100 mM NaCl, 1 mM EDTA, 1.0% NP-40, 0.5% sodium deoxycholate, 1 mM Na_3VO_4, 40 μg/ml PMSF), buffer B (10 mM Tris-HCl, pH 7.2, 1 M NaCl, 1 mM EDTA, 0.1% NP-40, 1 mM Na_3VO_4, 40 μg/ml PMSF), ST (see above), and 1× kinase buffer (20 mM HEPES, pH 7.2, 100 mM $MgCl_2$, 1 mg/ml bovine serum albumin). Immune complexes were then resuspended in 20 μl 1.5× kinase buffer. Kinase reactions were initiated with the addition of 10 μl of "start" solution containing cold ATP (50 μM final), [^{32}P]ATP (10 μCi/reaction mixture), cyclic AMP-dependent protein kinase inhibitor (0.03 μg/reaction mixture; Sigma), and recombinant glutathione *S*-transferase (GST)–S6 purified from bacteria (2 μg/reaction mixture) and incubated at 30°C for 10 min. Kinase reactions were terminated by the addition of 30 μl of 2× sample buffer. The amount of ^{32}P incorporated into GST-S6 was measured using a PhosphorImager (Typhoon 9400; Amersham Biosciences) and quantitated using the software ImageQuant TL.

Flow cytometry to determine relative cell size. HEK293 cells on 60-mm plates (80% confluent) were cotransfected with 1 μg green fluorescent protein (GFP)-spectrin and 10 μg Myc-mTOR plasmids. The next day, one-quarter of a 60-mm plate was transferred to a 10-cm plate and allowed to proliferate in DMEM-FBS in the absence or presence of rapamycin (20 ng/ml) for 72 h. For immunoblot analysis, one-half of the 60-mm culture was plated to a 10-cm plate and cultured for ~24 h. For cell size analysis, plates of subconfluent cells were washed once with PBS and incubated in 3 ml PBS–0.1% EDTA for ~5 min at room temperature. Cells were then gently triturated off the plastic and transferred to conical tubes on ice, centrifuged for 5 min at 1,000 rpm, and washed with 3 ml of PBS–1% calf serum. Cells were again centrifuged at 1,000 rpm for 5 min, resuspended in 0.5 ml PBS, fixed in 80% ethanol by adding 5 ml 88% ethanol, and stored overnight at 4°C. Immediately before fluorescence-activated cell sorting analysis, fixed cells were centrifuged at 1,600 rpm for 5 min, washed in 3 ml PBS–1% calf serum, and centrifuged at 1,000 rpm for 5 min. DNA was stained by resuspending fixed cells in 1 to 1.5 ml PI-RNase A solution and incubating them at 37°C for 30 min. The PI-RNase A solution contained the following: 10 μg/ml propidium iodide in 0.76 mM sodium citrate (pH 7.0), 250 μg/ml RNase A in 10 mM Tris-HCl (pH 7.5), 15 mM NaCl diluted in PBS–1% calf serum. For cell size analysis by flow cytometry, the mean forward scatter height (FSC-H) of 5,000 GFP-positive, G_1-phase cells was determined by gating on GFP and PI fluorescence using a BD Biosciences FACSCalibur with CellQuest software.

Image editing. For some figures, irrelevant lanes were removed from a scanned autoradiograph and flanking lanes juxtaposed using Adobe Photoshop. The presence of a thin, vertical black line indicates such a modification.

Statistical analyses. To quantitate ECL Western blot band densities, the software NIH Image J (version 1.41) was used after scanning/digitizing the autorads; a Student's unpaired *t* test (two-sample, assuming equal variances; two tails) was used (a *P* value of <0.05 was considered significant). For the cell size experiments, analysis of variance (ANOVA) followed by Tukey's post hoc tests was used to determine the significance of the population means (a *P* value of <0.01 was considered significant). The software Prism 5 from GraphPad was used for the ANOVA.

RESULTS

Identification of S1261 as a novel phosphorylation site on mTOR by mass spectrometry. While growth factors, mitogens, and nutrients upregulate mTORC1 signaling, the biochemical mechanisms by which these stimuli directly activate mTORC1 remain unclear. As reversible protein phosphorylation controls the function of many signaling intermediates in the mTORC1

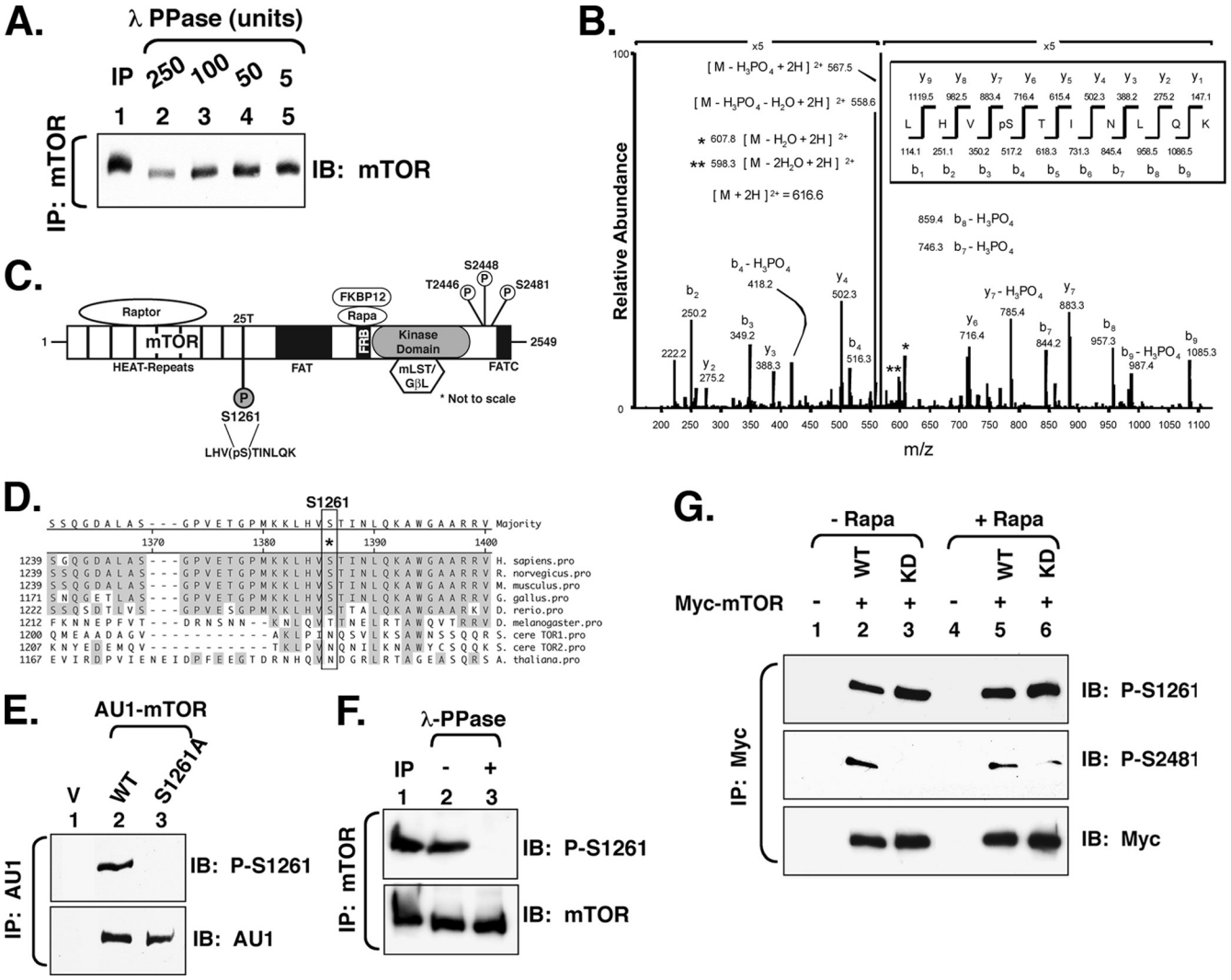

FIG. 1. Identification of S1261 as a novel in vivo mTOR phosphorylation site in intact cells. (A) mTOR undergoes extensive phosphorylation in vivo. HEK293 cells cultured in DMEM-FBS (steady state) were lysed in CHAPS buffer, and mTOR was immunoprecipitated. Immunoprecipitates were either resuspended immediately in sample buffer (IP) or washed in phosphatase buffer and incubated in vitro with various units of λ-phosphatase, resolved on 6% SDS-PAGE, and immunoblotted as indicated (IB). (B) Low-energy collision-induced dissociation spectrum of the doubly charged mTOR pS1261 phosphopeptide. HEK293 cells were transfected with AU1-mTOR, cultured in DMEM-FBS, lysed in CHAPS buffer, and immunoprecipitated with AU1 antibodies. A Coomassie-stained band of AU1-mTOR was digested with trypsin after SDS-PAGE. Liquid chromatography-MS/MS and data analysis were conducted as described in Materials and Methods. Note that the y_6 singly charged ion distinguishes between phosphorylation at S1261 and T1262. (C) Localization of P-S1261 and previously identified P-sites within mTOR's domain structure (4). S1261 maps to a central region of mTOR within HEAT repeat unit 25T, which lies N-terminal to the FAT domain (48), while T2446, S2448, and S2481 lie in the extreme C terminus after the FRB and kinase domains but prior to the FATC domain (7, 43, 49). The tryptic peptide in which P-S1261 was identified is shown. (D) Alignment of mTOR S1261 from various organisms using the algorithm Clustal W. The *Caenorhabditis elegans* sequence was omitted due to poor alignment resulting from large regions of nonhomology. (E) P-S1261 antibodies are site specific. HEK293 cells were transfected with vector control (V) or with WT or S1261A AU1-mTOR alleles, as indicated, and lysed in CHAPS buffer. WCL were immunoprecipitated with AU1 antibodies and immunoblotted with the indicated antibodies. (F) P-S1261 antibodies are phospho-specific. mTOR immunoprecipitates from HEK293 cells (lysed in CHAPS buffer) were either resuspended immediately in sample buffer (IP) or washed in phosphatase buffer and incubated in the absence or presence of λ-phosphatase (250 units). The immunoprecipitates were immunoblotted as indicated. (G) S1261 is not an autophosphorylation site. HEK293 cells were transfected with vector control, WT (1.0 μg), or KD (1.0 μg) Myc-mTOR plasmids and incubated in the absence or presence of rapamycin (20 ng/ml) for 2 h. Cells were lysed in CHAPS buffer, and WCLs were immunoprecipitated with Myc antibodies and immunoblotted as indicated.

pathway, we examined the phosphorylation of mTOR itself. Indeed, λ-phosphatase treatment of mTOR increased its mobility on SDS-PAGE (Fig. 1A), suggesting the extensive phosphorylation of mTOR in vivo. We used liquid chromatography-MS/MS to identify novel in vivo phosphorylation sites (P-sites) on AU1-tagged mTOR immunoprecipitated from transiently transfected HEK293 cells. Serine 1261 was identified as an unambiguous site of mTOR phosphorylation in cells growing in serum-containing medium as well as in factor-deprived cells that were stimulated with both insulin and amino acids (Fig.

1B). While this work was in preparation, Daub et al. also identified S1261 as a site of mTOR phosphorylation in intact cells in a MS/MS-based phospho-proteomic screen, further confirming S1261 as a novel mTOR phosphorylation site (11a). Notably, our analysis identified two of the three previously identified P-sites that localize to the C terminus of mTOR-S2448 (a site phosphorylated by S6K1 via a feedback loop) and S2481 (a site of autophosphorylation) (8, 25, 43, 49) (data not shown). S1261 lies within HEAT-repeat motif 25T in the middle of mTOR (Fig. 1C) (48) and is conserved among animals (human, rat, mouse, chick, zebrafish, and fly [in which it contains Thr rather than Ser]) but not in yeast or plants (*Arabidopsis*) (Fig. 1D). To confirm mTOR S1261 phosphorylation (P-S1261) in vivo and to facilitate the study of P-S1261 regulation, we generated rabbit polyclonal, affinity-purified antibodies using an mTOR peptide phosphorylated on S1261. This antibody recognized WT AU1-mTOR but not an AU1-mTOR phosphorylation site-defective mutant bearing an Ala substitution for S1261 (S1261A) (Fig. 1E). Additionally, P-S1261 antibodies failed to recognize λ-phosphatase-treated endogenous mTOR (Fig. 1F). Taken together, these data demonstrate the site and phosphorylation state specificity of the P-S1261 antibody.

With this antibody in hand, we first asked whether S1261 is a site of autophosphorylation, similar to S2481. Consistent with published data (49), exogenously expressed, Myc-tagged WT-mTOR autophosphorylated on S2481 while KD-mTOR did not (Fig. 1G). As both WT- and KD-mTOR exhibited similar S1261 phosphorylation, these data suggested that an autophosphorylation mechanism does not mediate mTOR P-S1261. Similar results were obtained using AU1-tagged mTOR alleles (data not shown). As mTORCs reportedly dimerize (71, 75), we next sought to exclude the possibility that P-S1261 occurs on KD-mTOR when a TORC containing endogenous WT-mTOR phosphorylates a TORC containing exogenous KD-mTOR via a *trans*-autophosphorylation mechanism. We thus pretreated cells with rapamycin in order to inhibit the activity of endogenous mTORC1 and found that rapamycin had no effect on P-S1261 on KD-mTOR, thus supporting the conclusion that S1261 is not a site of mTOR autophosphorylation (Fig. 1G).

Insulin/PI3K signaling promotes mTOR S1261 phosphorylation in both mTORC1 and mTORC2. As insulin stimulates mTORC1 and mTORC2 signaling (4, 31), we examined whether insulin signaling promotes mTOR P-S1261 in mTORC1 and mTORC2 in 3T3-L1 adipocytes, a classic insulin-responsive cell line. To examine P-S1261 in TORC1 versus TORC2, we immunoprecipitated raptor or rictor, respectively, as these partners uniquely define the complex. In mTORC1, insulin increased P-S1261 on raptor-associated mTOR, and pretreatment with the PI3K inhibitor wortmannin inhibited this insulin-induced increase (Fig. 2A, left panel). In this experiment, we were unable to determine the sensitivity of P-S1261 to rapamycin, as rapamycin pretreatment resulted in the partial dissociation of mTOR from raptor, as reported previously (46), making analysis of the degree of mTOR P-S1261 in mTORC1 difficult to assess accurately. HEK293 experiments described below (Fig. 2C), in which the levels of raptor-associated mTOR in the absence and presence of rapamycin were similar, suggest that mTOR P-S1261 in mTORC1 is insensitive to rapamycin. In mTOR immunoprecipitates, which contain a mixture of TORC1, TORC2, and possibly other not-yet-identified mTOR complexes, insulin increased P-S1261 in a wortmannin-sensitive but rapamycin-insensitive manner (Fig. 2B, right panel). In mTORC2, insulin also increased P-S1261 on rictor-associated mTOR in a wortmannin-sensitive but rapamycin-resistant manner (Fig. 2B). Collectively, these data show that in 3T3-L1 adipocytes, insulin/PI3K signaling promotes mTOR P-S1261 in both mTORC1 and mTORC2 in a rapamycin-insensitive manner.

As mTORC1 signaling has been extensively studied in HEK293 cells, the cell type in which we identified P-S1261, we also analyzed the regulation of P-S1261 in this cell type. While we have found it difficult to observe an insulin-induced increase in P-S1261 on mTOR associated with endogenous raptor (due to high basal P-S1261), coimmunoprecipitation of endogenous mTOR with exogenously expressed Myc-raptor revealed that in HEK293 cells, as in 3T3-L1 adipocytes, insulin promotes mTOR P-S1261 in a wortmannin-sensitive and thus PI3K-dependent manner (Fig. 2B, left panel). In certain experiments, the rapamycin sensitivity of P-S1261 in mTORC1 could not be assessed accurately (e.g., experiment 1 in Fig. 3A, left panel) due to rapamycin-induced dissociation of mTOR from Myc-raptor (46). In certain experiments where rapamycin failed to dissociate mTOR from raptor (e.g., experiment 2 in Fig. 3A, right panel), we found that rapamycin has no effect on the phosphorylation of mTOR S1261 in mTORC1. Taken together, these data indicate that insulin promotes mTOR P-S1261 in mTORC1 and mTORC2 in a PI3K-dependent and rapamycin-insensitive manner in HEK293 cells and 3T3-L1 adipocytes. The remainder of the work presented here focuses on the regulation and function of mTOR P-S1261 in mTORC1.

As sufficient levels of amino acids are required for mTORC1 signaling, we investigated a role for amino acids in modulation of TOR P-S1261. HEK293 cells expressing exogenous Myc-raptor were cultured under steady-state conditions or incubated in D-PBS–glucose for 1 h (to effect amino acid deprivation). As expected, withdrawal of amino acids from the medium downregulated mTORC1 signaling, as shown by the dephosphorylation of the ribosomal protein S6 (Fig. 2D). We found that withdrawal of amino acids from the medium resulted in reduced P-S1261 on Myc-raptor-associated mTOR (Fig. 2D). These data indicate that maintenance of mTOR S1261 phosphorylation requires amino acids and are consistent with the idea that amino acid sufficiency primes mTORC1 for subsequent growth factor-mediated S1261 phosphorylation and activation.

TSC inhibits and Rheb promotes mTOR S1261 phosphorylation in mTORC1. Inactivation of the TSC tumor suppressor via mutation of either the *TSC1* or *TSC2* genes leads to constitutively high mTORC1 signaling (27). To determine if TSC suppresses mTOR P-S1261, we examined P-S1261 in 3T3-immortalized, TSC1 null MEFs (37). As for the phosphorylation of the mTORC1-dependent substrates S6K1 and the ribosomal protein S6, P-S1261 on raptor-associated mTOR was significantly higher in $TSC1^{-/-}$ cells compared to wild-type cells in the absence of serum growth factors (Fig. 3A). Thus, TSC negatively regulates mTOR S1261 phosphorylation in mTORC1. We also examined a role for amino acids in the maintenance of

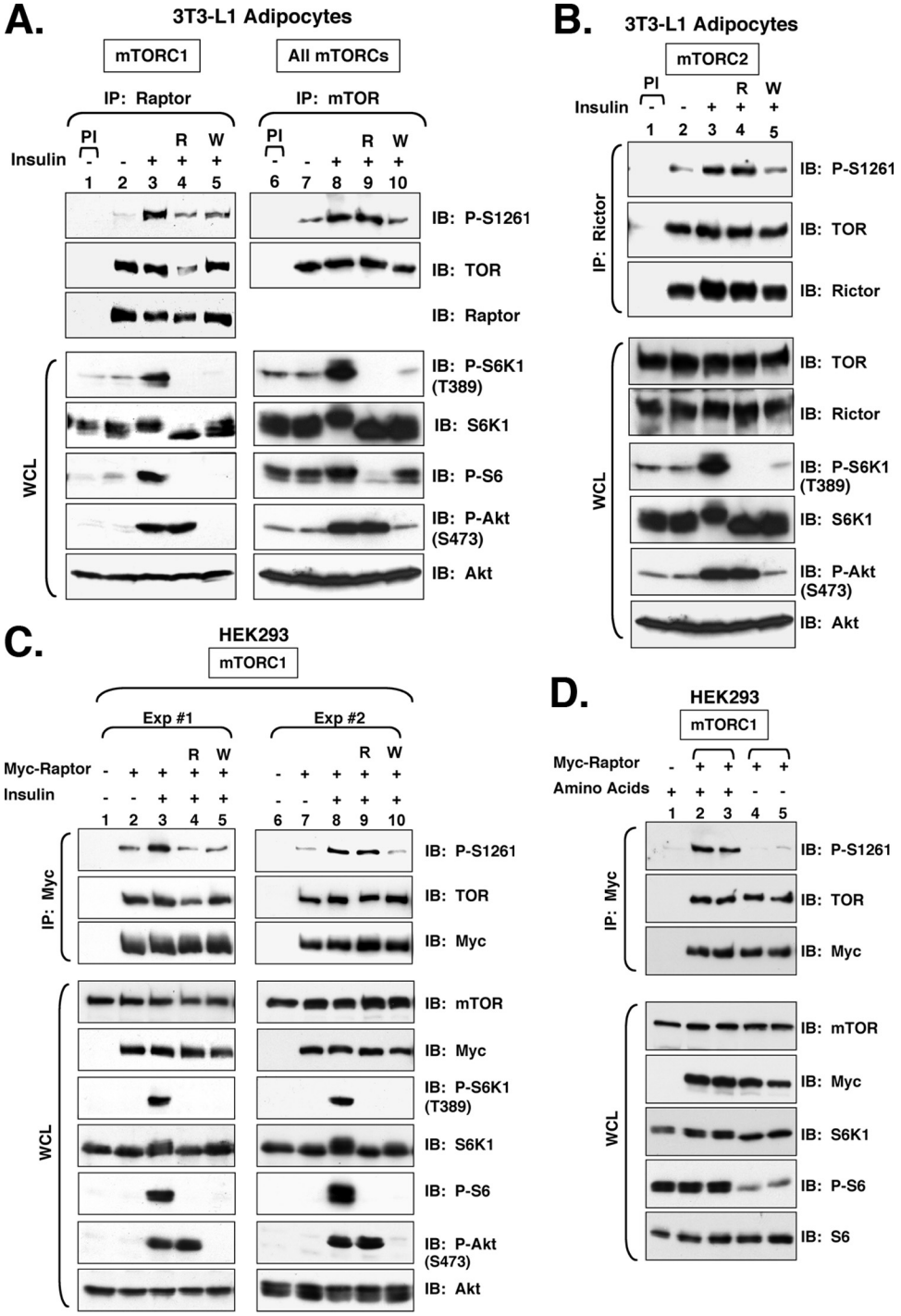

FIG. 2. Insulin stimulates mTOR S1261 phosphorylation in mTORC1 and mTORC2. (A) Regulation of mTORC1-associated mTOR P-S1261 in 3T3-L1 adipocytes: Adipocytes were serum deprived (24 h), pretreated with rapamycin (R; 20 ng/ml), or wortmannin (W; 100 nM) for 30 min, incubated in the absence or presence of insulin (100 nM) for 30 min, and lysed in CHAPS buffer. WCL were immunoprecipitated with preimmune sera (PI), raptor antibodies (left panel), and mTOR antibodies (right panel) (IP). Immunoprecipitates were immunoblotted as indicated (upper panels), and WCL was immunoblotted to confirm the expected activation and/or inhibition of mTORC1 signaling by the various treatments (lower panels) (IB). Note: the left and right panels represent independent experiments. (B) Regulation of mTORC2-associated mTOR P-S1261 in 3T3-L1 adipocytes. Adipocytes were treated, lysed, and analyzed as described above, except that rictor antibody was used for immunoprecipitation to isolate mTORC2. (C) Regulation of mTOR P-S1261 in HEK293 cells. Cells were transfected with vector control or with Myc-raptor (0.5 μg) and serum deprived (24 h). Cells were pretreated with rapamycin (R; 20 ng/ml), and wortmannin (W; 100 nM), incubated in the absence or presence of insulin (100 nM) for 30 min, and lysed in CHAPS buffer. WCL were immunoprecipitated with Myc antibodies (lanes 1 to 10). Immunoprecipitates (upper panels) and WCL (lower panels) were immunoblotted (IB) as indicated. Note: the left and right panels represent two distinct experiments that were performed identically. On the left, rapamycin partially dissociated mTOR from raptor, while in the experiment shown on the right, rapamycin failed to dissociate mTOR from raptor. While rapamycin dissociated mTOR from raptor in a majority of experiments, a minority failed to show such dissociation, for reasons unclear to us. (D) Amino acids are required to maintain mTOR P-S1261 in mTORC1 in HEK293 cells. HEK293 cells were transfected with Myc-raptor (0.5 μg) and cultured under steady-state conditions. Amino acids were withdrawn via incubation in D-PBS/Glc for 60 min. Myc-raptor was immunoprecipitated, and the level of P-S1261 on Myc-raptor-associated mTOR was assessed by immunoblotting. WCL was immunoblotted as indicated.

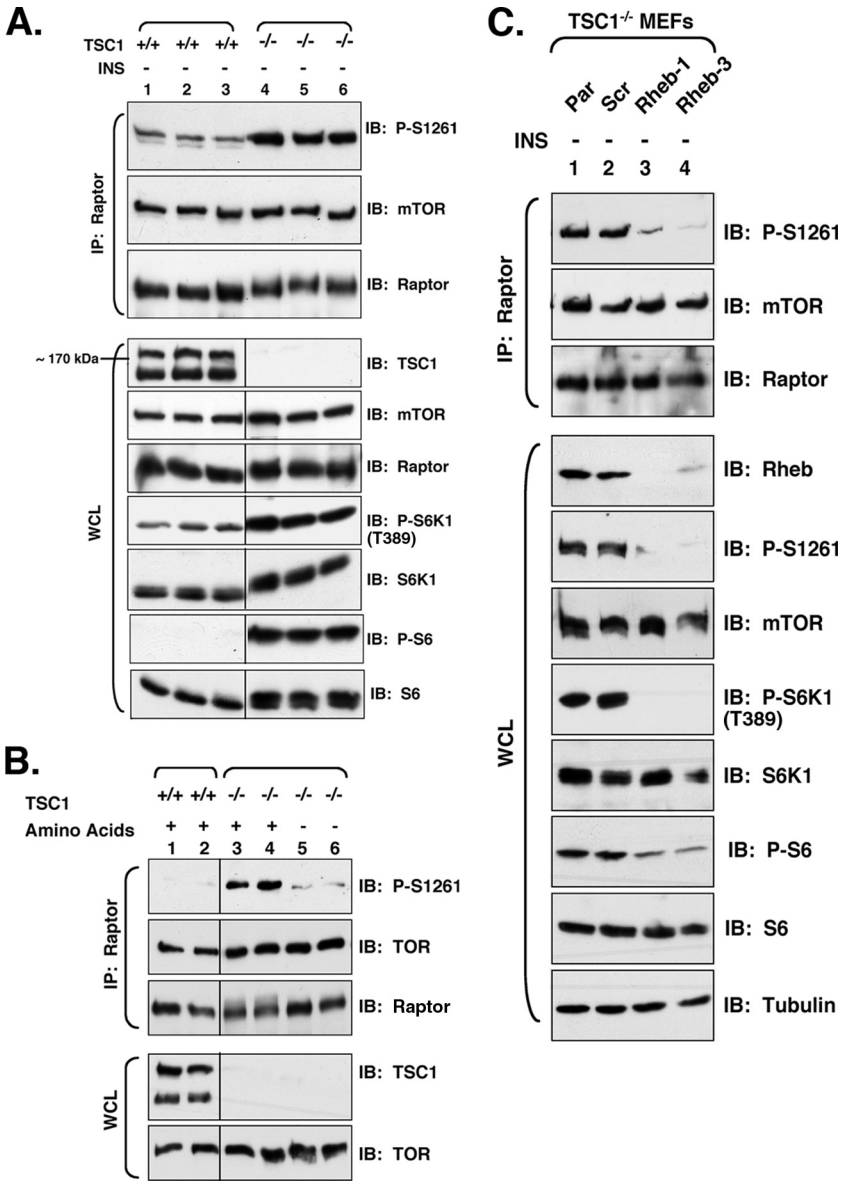

FIG. 3. TSC inhibits and Rheb promotes mTOR P-S1261. (A) TSC1$^{-/-}$ MEFs exhibit high levels of mTORC1-associated mTOR P-S1261 compared to WT MEFs. Littermate-matched, 3T3 immortalized mouse embryonic fibroblasts derived from TSC1$^{+/+}$ or TSC$^{-/-}$ animals were serum deprived (24 h) and lysed in CHAPS buffer. Triplicate lysates were immunoprecipitated with raptor antibodies and immunoblotted as indicated. Note: as we found that TSC1$^{-/-}$ fibroblasts express higher levels of total raptor and mTOR protein, two-thirds of the immunoprecipitate from TSC1$^{-/-}$ cells was loaded relative to that for TSC1$^{+/+}$ cells in order to normalize the amounts of raptor and mTOR between the two cell lines. WCL were loaded similarly. (B) Amino acids are required to maintain mTORC1-associated mTOR P-S1261 in TSC1$^{-/-}$ MEFs. Littermate-matched, TSC1$^{+/+}$, and TSC1$^{-/-}$ MEFs were cultured under steady-state conditions. TSC1$^{-/-}$ MEFs were also amino acid deprived by incubation in D-PBS/Glc for 60 min. Raptor was immunoprecipitated, and the level of P-S1261 on raptor-associated mTOR was assessed by immunoblotting (IB). WCL were immunoblotted as indicated. (C) Knockdown of Rheb in TSC1$^{-/-}$ MEFs reduces mTORC1-associated mTOR P-S1261. Parental TSC1$^{-/-}$ MEFs (Par) were infected with a control scrambled shRNA lentivirus (Scr) or with shRNA lentiviruses targeting two distinct regions of Rheb (Rheb-1 and Rheb-3). Infected cells were selected in puromycin and serum deprived. Raptor was immunoprecipitated, and the level of P-S1261 on raptor-associated mTOR was assessed by immunoblotting. WCL were immunoblotted to confirm Rheb knockdown and the expected decrease in mTORC1 signaling as well as to observe the level of P-S1261 on total mTOR.

mTOR P-S1261 in mTORC1 isolated from TSC1$^{-/-}$ fibroblasts. We found that withdrawal of amino acids from cycling TSC1$^{-/-}$ fibroblasts decreased the level of raptor-associated mTOR P-S1261 (Fig. 3B). Thus, sufficient levels of amino acids are required to maintain mTOR P-S1261 in mTORC1 in both TSC null fibroblasts as well as HEK293 cells. To determine whether Rheb is required for mTOR S1261 phosphorylation, we knocked down Rheb by infecting TSC1$^{-/-}$ MEFs with lentiviruses encoding shRNA hairpins targeting two distinct Rheb sequences. Parental TSC1$^{-/-}$ MEFs as well as those infected with scrambled control, Rheb-1, and Rheb-3 lentiviruses were serum deprived, and S1261 phosphorylation status

on raptor-associated mTOR was examined by coimmunoprecipitation and on total mTOR by immunoblotting of whole-cell lysate. As expected, parental TSC1$^{-/-}$ fibroblasts as well as those infected with the scrambled shRNA exhibited strong phosphorylation of S6K1 and S6 as well as strong raptor-associated and total mTOR P-S1261. TSC1$^{-/-}$ MEFs with reduced Rheb expression, however, exhibited the expected reduction in S6K1 and S6 phosphorylation, and raptor-associated and total mTOR P-S1261 were reduced as well (Fig. 3C). These data demonstrate that phosphorylation of mTOR S1261 in mTORC1 requires Rheb.

Phosphorylation of mTOR on S1261 promotes mTORC1-mediated phosphorylation and activation of S6K1. As no evidence currently exists to support a role for site-specific mTOR phosphorylation in regulation of mTORC1 signaling, we asked whether mTOR S1261 phosphorylation regulates mTORC1-mediated phosphorylation S6K1 on its hydrophobic motif site, T389. We took advantage of an RR mutant of mTOR that contains a point mutation (S2035I) in the FRB (FKBP12/rapamycin binding) domain, rendering the FKBP12/rapamycin complex unable to bind to and inhibit mTOR as part of mTORC1 (6, 9, 60). Thus, the use of RR-mTOR in conjunction with rapamycin permits the study of in vivo signaling by exogenously expressed mTOR isoforms in the absence of signaling by endogenous mTORC1. We compared the ability of RR and various RR/mutant AU1-mTOR isoforms to mediate the phosphorylation of cotransfected HA-S6K1 on T389 in the presence of rapamycin. As expected, rapamycin inhibited the phosphorylation of immunoprecipitated HA-S6K1 in cells that coexpressed WT-mTOR, expression of RR-mTOR rescued the rapamycin-mediated inhibition of HA-S6K1 phosphorylation, and a RR-mTOR allele bearing a kinase dead mutation (RR/KD) failed to rescue HA-S6K1 phosphorylation. Under either steady-state conditions (Fig. 4A) or in response to acute insulin stimulation after growth factor deprivation (Fig. 4B), the phosphorylation of HA-S6K1 on T389 was impaired in cells expressing RR/S1261A-mTOR relative to those expressing RR-mTOR. Under both conditions, S6K1 phosphorylation was reduced ~60% in cells expressing RR/S1261A-mTOR relative to those expressing RR-mTOR. We also assayed the ability of RR versus RR/S1261A mTOR to rescue rapamycin-induced inhibition of S6K1 activity by in vitro immune complex kinase assay using recombinant GST-S6 as substrate and [^{32}P]ATP. Consistent with the decreased ability of RR/S1261A-mTOR to phosphorylate HA-S6K1 in vivo, HA-S6K1 immunoprecipitated from cells expressing RR/S1261A-mTOR was defective (~40%) in mediating the phosphorylation of GST-S6 in vitro compared to RR-mTOR (Fig. 4C). Consistently, in vivo phosphorylation of endogenous ribosomal protein S6 was also reduced in response to RR/S1261A-mTOR signaling (Fig. 4C). Together, these data indicate that the phosphorylation of mTOR S1261 contributes to the overall signaling capacity of mTORC1 toward S6K1.

Overexpression of Rheb activates mTORC1 signaling in the absence of serum growth factors (2, 19, 65). To determine whether phosphorylation of mTOR S1261 is required for Rheb-mediated activation of mTORC1 signaling, we compared the ability of RR-mTOR versus RR/S1261A-AU1-mTOR to mediate the phosphorylation of cotransfected HA-S6K1 in response to Rheb in the presence of rapamycin and absence of serum growth factors. As expected, overexpression of Rheb in serum-deprived cells led to a striking increase in phosphorylation of HA-S6K1 on T389, rapamycin completely inhibited this response, and coexpression with RR-mTOR rescued the rapamycin-mediated inhibition of P-S6K1 in response to Rheb overexpression (Fig. 4D). Cells expressing Rheb and RR/S1261A-AU1-mTOR exhibited impaired phosphorylation of HA-S6K1 compared to those expressing Rheb and RR-mTOR (Fig. 4D). These data reveal that phosphorylation of mTOR S1261 is required for Rheb-driven mTORC1 signaling. Lastly, we investigated whether RR-mTOR bearing a phospho-mimetic substitution at 1261 (S1261D) was sufficient to promote mTORC1 signaling to S6K1 in the absence of serum growth factors. We found that expression of RR/S1261D-mTOR in the presence of rapamycin failed to increase the phosphorylation of cotransfected HA-S6K1 in the absence of serum growth factors (Fig. 4E). These data suggest that the phospho-mimetic Asp substitution at S1261 does not sufficiently mimic phosphorylation to promote insulin-stimulated S6K1 phosphorylation in the absence of other growth factor signals.

Phosphorylation of mTOR on S1261 promotes mTORC1-mediated phosphorylation of 4EBP1. Insulin promotes mTORC1-dependent phosphorylation of 4EBP1, which contributes to initiation of cap-dependent translation (40). Two phosphorylation sites on 4EBP1 exhibit sensitivity to rapamycin (Ser 65 and Thr 70), while two others (Thr 37 and Thr 46) exhibit partial sensitivity (40). We therefore assayed the ability of RR versus RR/S1261A-mTOR to mediate the phosphorylation of cotransfected 3HA-4EBP1 on T70, S65, and T37/46 in the presence of rapamycin in response to insulin (Fig. 5). As expected, rapamycin reduced the insulin-stimulated phosphorylation of 4EBP1 on T70, S65, and T37/46 in cells coexpressing WT-mTOR, expression of RR-mTOR rescued this rapamycin-mediated inhibition of 4EBP1 phosphorylation, and expression of RR/KD failed to rescue the phosphorylation of these sites. We observed impaired phosphorylation of 4EBP1 on all three sets of sites (e.g., T70, S65, and T36/46) in cells expressing RR/S1261A-mTOR, which was most apparent on endogenous 4EBP1 and similar to the level of phosphorylation observed in cells expressing RR/KD-mTOR. These data indicate that phosphorylation of mTOR S1261 contributes to mTORC1-mediated phosphorylation of 4EBP1 in vivo.

S1261 phosphorylation promotes mTORC1 autokinase activity in vivo. To explore the mechanism by which P-S1261 promotes mTORC1 signaling, we examined the phosphorylation state of the mTOR S2481 autophosphorylation site in order to examine the effect of P-S1261 on mTORC1's intrinsic in vivo kinase activity. As the original characterization of P-S2481 occurred before the existence of different mTOR complexes was known (49), we first characterized the regulation of P-S2481 in response to insulin and Rheb overexpression specifically in mTORC1. We thus cotransfected HEK293 cells with Myc-raptor and AU1-mTOR in the absence and presence of Flag-Rheb and cultured the cells in the absence or presence of insulin and wortmannin. Insulin promoted a wortmannin-sensitive increase in P-S2481 on Myc-raptor-associated mTOR, and Rheb overexpression strongly increased the P-S2481 signal (Fig. 6A). These data demonstrate that insulin/PI3K/Rheb signaling promotes mTOR S2481 autophosphoryla-

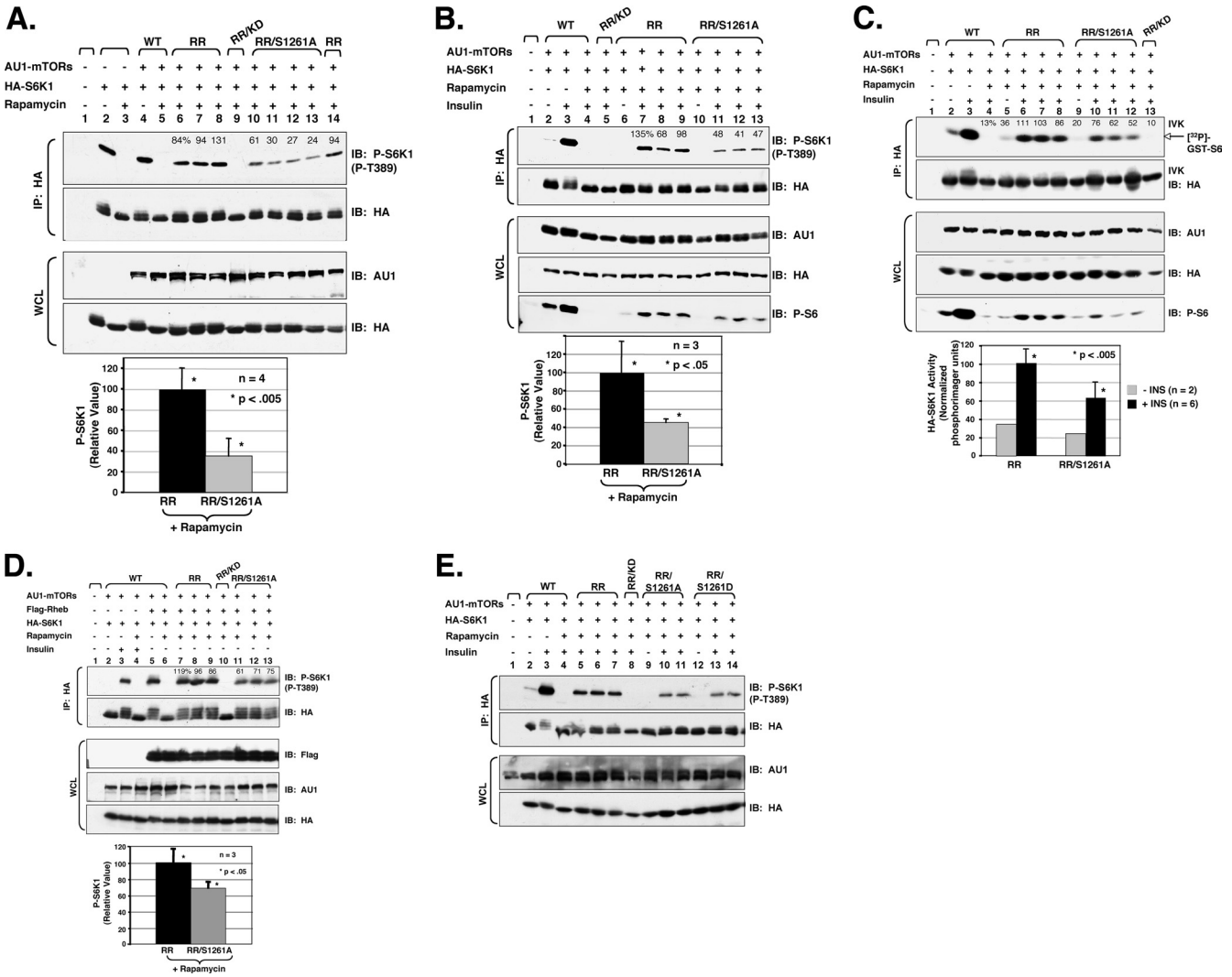

FIG. 4. Phosphorylation of mTOR S1261 promotes mTORC1-mediated phosphorylation and activation of S6K1. (A) P-S1261 promotes S6K1 phosphorylation under steady-state conditions. HEK293 cells were transiently transfected with vector control or cotransfected with HA-S6K1 (0.5 μg) without or with various AU1-mTOR alleles (5 μg) as indicated and cultured in DMEM-FBS. Transfected cells were pretreated without or with rapamycin (20 ng/ml) for 2 h prior to lysis in NP-40–Brij buffer, where indicated. WCL were immunoprecipitated with HA antibodies and immunoblotted as indicated. WCL were also immunoblotted directly. To quantitate the level of S6K1 phosphorylation, the P-S6K1 signal was analyzed by densitometry. The numbers on the uppermost image indicate the densities (percentages) of each P-S6K1 band relative to the mean (set to 100%) of the four RR bands (lanes 6 to 8 and 14). The relative P-S6K1 signals in the graph were normalized to the total amount of HA-S6K1 in each immunoprecipitate (mean ± standard deviation). *, $P < 0.005$. (B) P-S1261 promotes S6K1 phosphorylation in response to insulin. Results are shown for an experiment similar to that shown in Fig. 3A except that transfected cells were serum deprived (24 h), pretreated without or with rapamycin (20 ng/ml) for 30 min, and then incubated in the absence or presence of insulin (100 nM) for 30 min, as indicated. (C) P-S1261 promotes S6K1 activation in response to insulin. Results are shown for an experiment similar to that shown in Fig. 3B above except that HEK293 cells were cotransfected with 0.2 μg HA-S6K1 together with 5 μg AU1-mTOR alleles. After HA-S6K1 immunoprecipitation, in vitro immune complex kinase (IVK) assays were performed using recombinant GST-S6 as substrate and [^{32}P]ATP. In vitro kinase reactions were resolved on SDS-PAGE. The portion of the gel containing HA-S6K1 was transferred to a PVDF membrane and immunoblotted with HA antibodies, while the portion of the gel containing GST-S6 was dried and exposed to a phosphorimager screen. The relative amount of radioactive ^{32}P added to GST-S6 by HA-S6K1 is shown by the numbers on the upper image. The mean activity of HA-S6K1 in response to insulin-stimulated RR-mTOR signaling was set to 100%, and all other activities are relative to this value. The graph in the lower panel shows the combined results of two independent experiments (mean ± standard deviation). The mean activity of HA-S6K1 in response to insulin-stimulated RR-mTOR signaling was set to 100%, and all other activities are relative to this value. *, $P < 0.005$ by unpaired t test. (D) P-S1261 is required for Rheb-driven S6K1 phosphorylation in the absence of serum growth factors. HEK293 cells were cotransfected with HA-S6K1 (0.5 μg) together with various AU1-mTOR alleles (2.5 μg) and Flag-Rheb (2.5 μg). Cells were serum deprived (24 h), pretreated without or with rapamycin (20 ng/ml) for 1 h, stimulated in the absence or presence of insulin (100 nM) for 30 min, and lysed in NP-40–Brij buffer, as indicated. WCL were immunoprecipitated with HA antibodies and immunoblotted, as indicated. WCL were also immunoblotted directly. (E) In the absence and presence of insulin, the S1261D allele does not behave in a phospho-mimetic manner. The experiment was performed similarly to that in panel B.

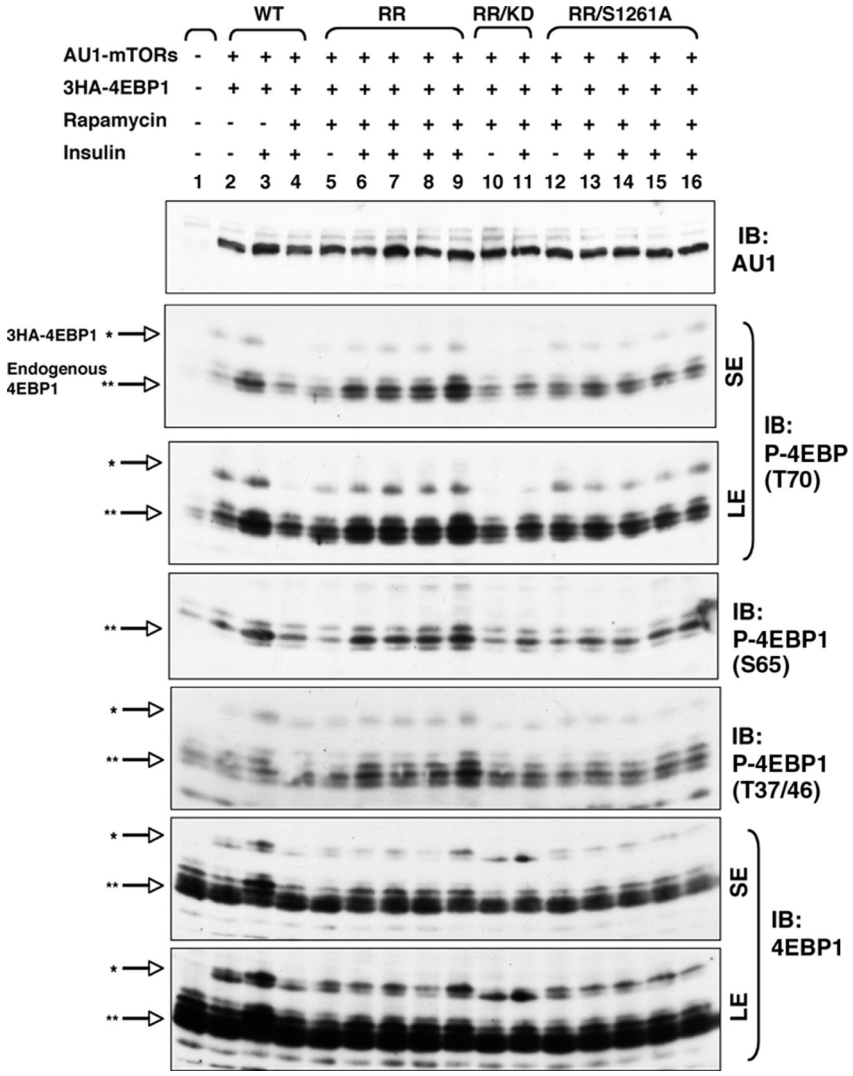

FIG. 5. Phosphorylation of mTOR S1261 promotes mTORC1-mediated 4EBP1 phosphorylation. HEK293 cells were transfected with various AU1-mTOR alleles (4 μg) together with 3HA-4EBP1 (1 μg), deprived of serum (24 h), pretreated without or with rapamycin (20 ng/ml) for 30 min, incubated in the absence or presence of insulin (100 nM) for 30 min, and lysed in NP-40–Brij buffer. WCL were resolved on SDS-PAGE and immunoblotted with the indicated antibodies. SE, short exposure; LE, long exposure. The positions of 3HA-4EBP1 (*) versus endogenous 4EBP1 (**) are indicated.

tion in mTORC1 and support the idea that P-S2481 reflects mTORC1's in vivo intrinsic catalytic activity. We next investigated the role of P-S1261 in regulation of mTORC1's intrinsic catalytic activity using P-S2481 as a readout. HEK293 cells were cotransfected with Myc-raptor and various AU1-mTOR alleles in the presence of Flag-Rheb, and Myc-raptor was immmunoprecipitated to detect the phosphorylation of S2481 on associated mTOR. As expected, P-S2481 was significantly reduced relative to WT-mTOR when mTORC1 contained KD- or S2481A-mTOR (Fig. 6B). Notably, we observed reduced P-S2481 when mTORC1 contained S1261A-mTOR compared to mTORC1 that contained WT-mTOR. These data reveal that phosphorylation of mTOR S1261 contributes to the activation of mTORC1's in vivo intrinsic catalytic activity. Additionally, we found that the absence of TSC1 (Fig. 3A) or overexpression of Rheb (Fig. 6B) retarded the mobility of raptor on SDS-PAGE. Moreover, the Rheb-induced mobility shift of Myc-raptor was significantly reduced when mTORC1 contained KD-mTOR (Fig. 6B). These data suggest that in addition to promoting mTOR S1261 phosphorylation and S2481 autophosphorylation, TSC null status and Rheb promote extensive phosphorylation of raptor on many sites in a manner that requires mTORC1's kinase activity. These observations are consistent with recent reports demonstrating site-specific phosphorylation of raptor (5, 23, 70).

Since an altered interaction of raptor or mLST8/GβL with S1261A-mTOR could explain the defect in mTORC1 autophosphorylation or mTORC1-mediated substrate phosphorylation, we examined the coimmunoprecipitation of S1261A-mTOR with raptor and mLST/GβL. We cotransfected HEK293 cells with various isoforms of Myc-mTOR together with HA-raptor and HA-mLST/GβL. We found no difference in the ability of HA-raptor or HA-mLST8/GβL to coimmunoprecipitate with Myc-tagged S1261A-mTOR (in either the WT or RR backbones)

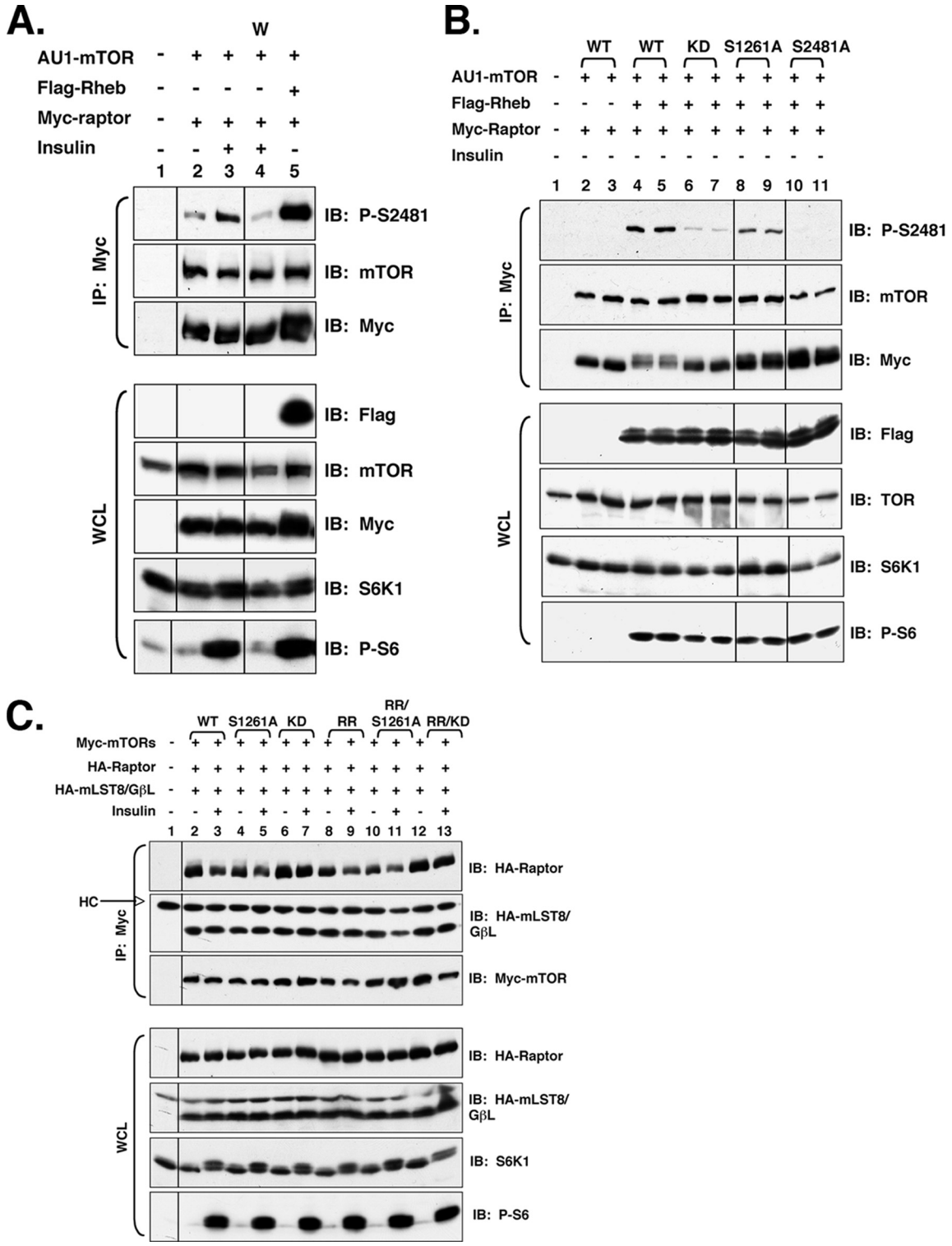

FIG. 6. mTOR S1261 phosphorylation is required for mTORC1's in vivo catalytic activity. (A) In mTORC1, S2481 autophosphorylation increases in response to insulin in a PI3K-dependent manner and upon Rheb overexpression. HEK293 cells were cotransfected with Myc-raptor (0.5 μg) together with Flag-Rheb (2.5 μg) and AU1-mTOR (2.5 μg), as indicated. Cells were serum deprived (24 h), pretreated with wortmannin (W; 100 nM), incubated in the absence or presence of insulin (100 nM), and lysed in NP-40–Brij buffer. WCL were immunoprecipitated with Myc antibodies and immunoblotted (IB) as indicated (upper panels). WCL were also immunoblotted (lower panels). (B) In mTORC1, P-S1261 is required for S2481 autophosphorylation. Results are for an experiment similar to that shown in panel A except that additional AU1-mTOR mutant alleles were cotransfected. (C) Phosphorylation of mTOR S1261 does not alter the interaction of mTOR with its TORC1 partners raptor and mLST8/GβL. HEK293 cells were cotransfected with HA-mLST8/GβL (0.5 μg) and HA-raptor (0.5 μg) together with various Myc-mTOR alleles (4 μg), cultured in DMEM-FBS, serum deprived (24 h), incubated in the absence or presence of insulin (100 nM), and lysed in CHAPS buffer. WCL were immunoprecipitated with anti-Myc antibodies and immunoblotted with the indicated antibodies.

compared to WT-mTOR (or RR-mTOR) under either steady-state conditions (data not shown) or in the absence or presence of insulin (Fig. 6C). Thus, phosphorylation of mTOR S1261 does not modulate the interaction of mTOR with its partners. Moreover, as S1261A-mTOR interacts with its partners normally, substitution of Ala for Ser at amino acid residue 1261 did not grossly impair mTOR's protein structure. We noted additionally that when we examined either transfected (Fig. 6C) or endogenous mTOR and raptor (data not shown), insulin mediated a moderately weakened interaction of raptor with mTOR while it had no effect on the interaction of mLST8/GβL with mTOR. This observation is reminiscent of the nutrient-regulated modulation of the mTOR-raptor interaction reported by Kim et al., who observed a weak mTOR-raptor interaction in nutrient-replete cells (high mTORC1 signaling) and a stronger mTOR-raptor interaction in nutrient-depleted cells (low mTORC1 signaling) (33). Taken together, these observations suggest that insulin as well as nutrients induce allosteric conformational changes in mTORC1 that affect the mTOR-raptor interaction and that may contribute to the regulation of mTORC1 signaling. Our data indicate that failure to phosphorylate S1261 is not sufficient to abrogate the insulin-induced weakening of the mTOR-raptor interaction.

Phosphorylation of S1261 on TOR promotes mTORC1-mediated cell growth. We reported previously that the level of mTORC1 signaling controls the size at which cells proliferate, which is a measure of the overall level of cell growth (16). To elucidate the molecular mechanisms underlying mTORC1-regulated cell growth, we asked whether S1261 phosphorylation plays a role in this major mTORC1 function. We therefore cotransfected HEK293 cells with GFP-tagged spectrin and a panel of Myc-tagged mTOR isoforms and used flow cytometry to measure the mean FSC-H (a measure of relative cell size) of the transfected (GFP-positive), G_1-phase population in the absence and presence of rapamycin. Combined cell size data from three experiments, each performed in quadruplicate (n = 12), are shown in Fig. 7A. As reported previously (16), inhibition of mTORC1 signaling with rapamycin under steady-state conditions decreased the mean FSC-H of cells expressing WT mTOR by ~10%, expression of RR-mTOR rescued the rapamycin-mediated decrease in cell size, and expression of RR/KD-mTOR failed to rescue the rapamycin-mediated decrease in cell size (Fig. 7A). Strikingly, cells expressing RR/S1261A-mTOR in the presence of rapamycin were statistically smaller than those expressing RR-mTOR, indicating a defect in the ability of RR/S1261A-mTOR to drive cell growth to increased cell size (Fig. 7A) (ANOVA followed by Tukey's post hoc tests confirmed the statistical significance of the FSC-H means). These data indicate that phosphorylation of mTOR S1261 contributes to mTORC1-driven cell growth. Interestingly, cells expressing the phospho-mimetic RR/S1261D allele exhibited a size that was statistically larger than those expressing RR/S1261A but not statistically as large as those expressing RR-mTOR. These data suggest that in cycling cells, the phospho-mimetic S1261D allele indeed mimics phosphorylation, albeit weakly. It is important to note that for each cell size experiment, we confirmed equal expression of the various Myc-mTOR alleles (the immunoblot corresponding to one representative cell size experiment is shown in Fig. 7A). To further analyze the ability of S1261D to mimic phosphorylation at S1261, we compared the ability of the Myc-tagged RR/S1261A versus RR/S1261D-mTOR alleles to rescue rapamycin-inhibited phosphorylation of S6K1 under steady-state conditions (as done for Fig. 4A) (Fig. 7B). As expected, RR-S1261A demonstrated impaired signaling to cotransfected HA-S6K1 compared to RR-mTOR. While the signaling capacity of RR/S1261D-mTOR was not statistically higher than RR/S1261A-mTOR, mean HA-S6K1 phosphorylation in cells expressing RR/S1261D was higher than in cells expressing RR/S1261A. These observations are consistent with the cell size data and suggest that the Asp (D) S1261 substitution weakly mimics phosphorylation.

DISCUSSION

Here we have elucidated the poorly understood mechanisms underlying mTORC1 regulation and provided the first evidence that site-specific mTOR phosphorylation (on S1261) regulates mTORC1 function. We show that insulin signals via PI3K to promote the autophosphorylation-independent (Fig. 1G), rapamycin-insensitive phosphorylation of mTOR S1261 in both mTORC1 and mTORC2 (Fig. 2A to C). Thus, mTOR S1261 phosphorylation is not mTOR complex specific. In mTORC1, maintenance of mTOR P-S1261 requires sufficient levels of amino acids in HEK293 cells and MEFs (Fig. 2D and 3B), similar to the requirement for amino acids in mTORC1-mediated substrate phosphorylation. As recent work suggests that amino acid sufficiency induces the subcellular relocalization of mTOR to a Rab7-positive endomembrane compartment that contains Rheb (52), an intriguing hypothesis presents itself: perhaps mTOR S1261 phosphorylation occurs in this unique Rheb-containing subcellular compartment. In the absence of amino acids, mTORC1 may relocalize out of this compartment, and thus S1261 phosphorylation could not be maintained. Moving downstream of PI3K, we find that TSC suppresses while Rheb promotes mTOR P-S1261, as fibroblasts lacking TSC1 exhibit elevated P-S1261 in the absence of serum growth factors (Fig. 3A) and Rheb knockdown reduces mTOR P-S1261 in TSC1 null MEFs (Fig. 3C). By using rapamycin-resistant mTOR alleles containing either wild-type or phosphorylation site-defective S1261 (S1261A) combined with rapamycin to inhibit signaling by endogenous mTORC1, we showed that mTOR P-S1261 is required for phosphorylation and activation of S6K1 and phosphorylation of 4EBP1 (Fig. 3A to C and 5). Thus, P-S1261 promotes mTORC1-mediated biochemical signaling to its best-characterized substrates. Additionally, Rheb-driven S6K1 phosphorylation (Fig. 3D), mTOR S2481 autophosphorylation in vivo (Fig. 6B), and mTORC1-driven cell growth (Fig. 7A) require P-S1261.

Based on our data, we propose the following simple model. Insulin signaling via PI3K mediates the TSC/Rheb-dependent phosphorylation of mTOR S1261, which contributes to activation of mTORC1's intrinsic catalytic activity (as measured by S2481 autophosphorylation) and thereby promotes mTORC1-mediated substrate phosphorylation (e.g., S6K1, 4EBP1), biochemical signaling, and cell growth (Fig. 8). Elucidation of the precise relationship between TSC/Rheb and mTOR P-S1261 awaits the identification and molecular cloning of the unknown P-S1261 regulator. While the model shown in Fig. 8 suggests that TSC/Rheb lies upstream of the P-S1261 regulator in a

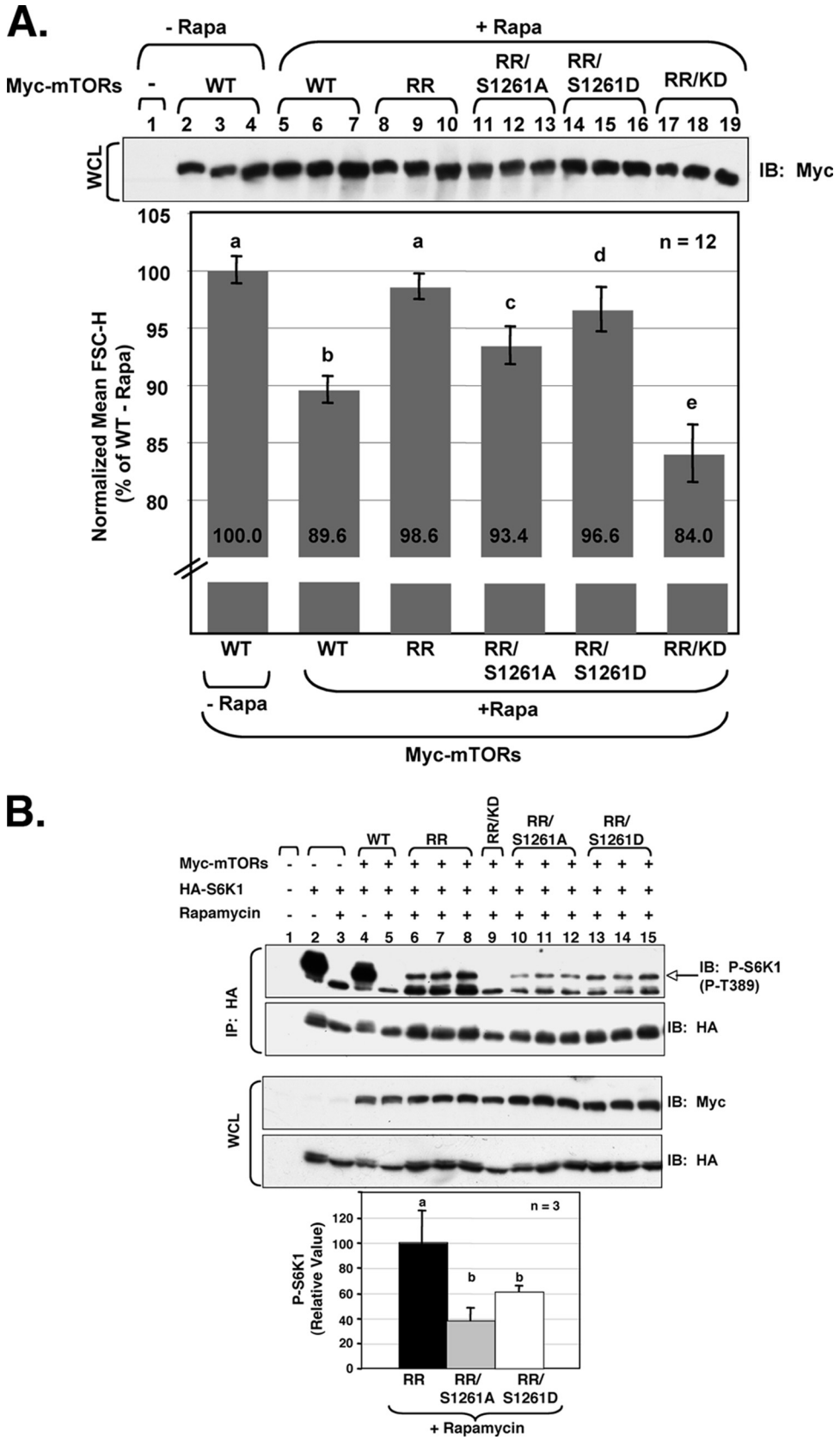

FIG. 7. Phosphorylation of mTOR S1261 promotes mTORC1-mediated cell growth with increased cell size. (A) Cells expressing RR/S1261A-mTOR exhibit impaired rescue of rapamycin-inhibited cell growth. HEK293 cells were cotransfected with GFP-spectrin (1 μg) together with various Myc-mTOR alleles (10 μg). One day posttransfection, the 60-mm plates were split to 10-cm plates and allowed to proliferate for 72 h in

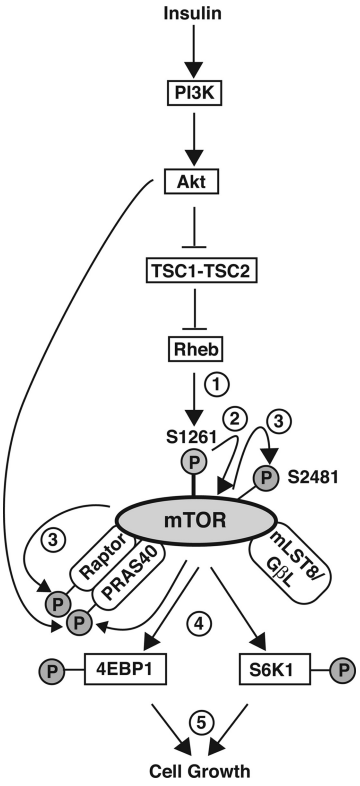

FIG. 8. Model for regulation of mTORC1 signaling by mTOR S1261 phosphorylation. We propose that insulin activates mTORC1 via a series of tightly regulated biochemical steps, allowing mTORC1 to respond appropriately to divergent and dynamic environmental cues. Insulin signals via PI3K and Akt to suppress TSC and thus activate Rheb. Akt directly phosphorylates TSC2 (27) and PRAS40 (54, 67) to cooperatively activate mTORC1. Insulin signaling via PI3K/TSC/Rheb promotes mTOR S1261 phosphorylation (step 1) (see Discussion for more details), which likely cooperates with other inputs to activate the mTORC1 kinase (step 2). Active mTORC1 phosphorylates itself (on S2481) as well as its partners (e.g., raptor [our data and reference 70] and PRAS40 [17, 45, 68]) (step 3), culminating in the phosphorylation of substrates (e.g., S6K1, 4EBP1) (step 4) and cell growth (step 5). Not shown is the recently described AMPK-mediated phosphorylation of raptor upon induction of energy stress (23) and the RSK-mediated phosphorylation of raptor upon mitogenic stimulation of the MAPK pathway (5), events that inhibit and activate mTORC1 signaling, respectively. Taken together, the emerging data suggest that multiple phosphorylation events on mTOR and its partners cooperate to regulate the activation state of mTORC1, both positively and negatively.

linear pathway in which Rheb modulates the activation state of the P-S1261 regulator, it is possible that TSC/Rheb and the P-S1261 regulator lie on parallel pathways that converge on mTORC1 to cooperatively activate the complex. Such an idea has precedent, as Akt mediates mTORC1 activation via parallel pathways, by the direct phosphorylation of TSC2, which activates Rheb (27), and by the direct phosphorylation of PRAS40, which relieves PRAS40's inhibitory effect on mTORC1 via induced dissociation (54, 67). It also remains unclear as to whether insulin promotes mTOR P-S1261 by modulating the action of a kinase or a phosphatase. The basic nature of the amino acids located in the S1261 consensus (KKLHVpS) suggests that a basophilic kinase mediates mTOR S1261 phosphorylation.

We are not the first to investigate the phosphorylation of mTOR. Prior to this work, three phosphorylation sites on mTOR had been identified: S2448, S2481, and T2446 (in order of discovery) (7, 43, 49). While S2448 was originally thought to be phosphorylated by Akt (43, 59), it is now believed that S6K1 mediates S2448 phosphorylation as part of a feedback loop whose function is currently unknown (8, 25). S2481 was identified as a site that underwent autophosphorylation in vitro and in vivo; additionally, growth factors were shown to weakly increase P-S2481 (49). This work proposed that P-S2481 is a measure of mTOR's in vivo autokinase activity (49). T2446 was identified as a site whose phosphorylation increased upon nutrient withdrawal (possibly via AMPK) and decreased upon insulin stimulation (7). Analysis of these phosphorylation sites failed to provide evidence that site-specific mTOR phosphorylation regulates mTOR signaling (49, 59). It is important to note, however, that the ability of mTOR to activate S6K1 was the only assay of mTOR function utilized in these studies. It remains possible, however, that these three P-sites participate in regulation of mTOR functions not yet identified, or alternatively, if several P-sites cooperatively regulate mTOR signaling, then analysis of individual P-sites may not be sufficient to observe a functionally defective phenotype. As our data reveal a modest defect in S1261A-mTOR signaling to mTORC1 substrates, an outstanding question remains as to whether P-S1261 cooperates with any of the three previously identified P-sites, or with other not-yet-identified P-sites, to coordinately regulate mTORC1 function.

Our data demonstrating that insulin/PI3K signaling and Rheb overexpression strongly promote mTOR S2481 autophosphorylation extend the work of Peterson et al. (49) and support a model whereby growth factors activate mTORC1 signaling by increasing mTORC1's intrinsic catalytic activity. This model has not had strong experimental support, however, as attempts to observe significant insulin-stimulated activation of mTORC1 by in vitro kinase assay have proven historically unsuccessful. Thus, it was postulated that insulin may activate mTORC1 signaling by a mechanism other than regulation of mTORC1's catalytic activity. Recently, however, Sancak et al.

the absence or presence of rapamycin. Relative size of subconfluent cells was determined using a flow cytometer and the parameter mean FSC-H. The graph in panel A shows the combined, mean FSC-H values (± standard deviations) of transfected (GFP-positive), G_1-phase cells from three experiments, each performed in quadruplicate ($n = 12$). The expression levels of the various Myc-mTOR alleles from one of the three experiments are shown (three of the four lysates are shown). The size of cells transfected with WT-mTOR and cultured in the absence of rapamycin was set at 100%. All other samples are shown relative to this value. Statistical significance was determined using a one-way ANOVA followed by Tukey's post hoc tests. The letters (a to d) indicate that the FSC-H means are significantly different at a P level of <0.01. (B) In cycling cells, the phospho-mimetic S1261D allele weakly mimics phosphorylation at S1261. The experiment was performed under steady-state conditions similar to the experiment shown in Fig. 4A except for the use of Myc-tagged mTORs.

(54) overcame technical problems inherent in commonly employed mTORC1 in vitro kinase assay protocols and demonstrated consequently that insulin greatly augments mTORC1's kinase activity, as assayed by in vitro phosphorylation of recombinant S6K1 and 4EBP1 (54). Furthermore, addition of recombinant Rheb-GTP to mTORC1 isolated from serum-deprived cells also potently activates mTORC1's in vitro kinase activity toward substrates (54). Collectively, the data demonstrating significant insulin-stimulated activation of mTORC1 kinase activity, as monitored by in vivo mTOR S2481 autophosphorylation (Fig. 6) and by in vitro kinase assay (54), support the notion that insulin increases mTORC1's kinase activity toward itself and toward exogenous substrates. As Rheb-driven mTOR S2481 autophosphorylation requires mTOR S1261 phosphorylation (Fig. 6B), these data indicate a role for mTOR S1261 phosphorylation in regulation of mTORC1's intrinsic catalytic activity.

In addition to our observations that phosphatase treatment increases mTOR's electrophoretic mobility on SDS-PAGE (Fig. 1A), which suggests the extensive phosphorylation of mTOR in vivo, we have also observed the extensive phosphorylation of raptor (Fig. 2C and 6B, our observations reported here, and also unpublished data). Consistent with these observations, recent work reports the phosphorylation of raptor: AMPK, a kinase activated by energy stress, directly phosphorylates raptor to attenuate mTORC1 signaling (23); RSK, a mitogen-activated kinase in the MAPK pathway, directly phosphorylates raptor to promote mTORC1 signaling (5); mTOR itself phosphorylates raptor to promote mTORC1 signaling (70). Moreover, several groups have reported that Akt and mTOR phosphorylate PRAS40, an mTORC1 interactor that displays properties of both an inhibitor and substrate, which results in the dissociation of PRAS40 from mTORC1 and promotes mTORC1 signaling to other substrates (e.g., S6K1 and 4EBP1) (17, 45, 54, 66–69). Collectively, these data suggest that multiple phosphorylation events on mTORC1 components (e.g., mTOR, raptor, PRAS40) cooperate to regulate mTORC1 signaling, thus ensuring precise mTORC1 regulation in response to diverse and dynamic environmental cues. It will be important in the future to identify the basophilic S1261 kinase, to determine whether P-S1261 cooperates with other P-sites on mTOR or its partners to regulate mTORC1 signaling, and to determine whether mTOR P-S1261 occurs in a distinct subcellular compartment. As insulin/PI3K signaling promotes mTOR P-S1261 in mTORC2, it will be critical to determine whether S1261 phosphorylation promotes mTORC2-mediated phosphorylation of Akt on its hydrophobic motif, S473, or the phosphorylation of other AGC kinase family members (e.g., PKCα, SGK1) on their respective hydrophobic motifs, S657 and S422 (1, 20, 26, 55, 56). Lastly, as mTOR S1261 phosphorylation does not appear to modulate the insulin-induced destabilization of the mTOR-raptor interaction (Fig. 6C), it will be important to identify the biochemical mechanism underlying this regulated interaction.

ACKNOWLEDGMENTS

We thank all members of the laboratory as well as Martin G. Myers, Jr., for critical reading of the manuscript. We are indebted to John Blenis for encouragement. Thanks go to David Sabatini, Robert Abraham, Nahum Sonenberg, Ormond MacDougald, David Kwiatkowski, and John Blenis for generously sharing reagents.

This work was supported by NIH R01 DK-078135, the American Diabetes Association, the American Cancer Society, and the Michigan Diabetes Research and Training Center (D.C.F.); the American Heart Association (G.A.S. and J.A.K.); and the Vermont Genetics Network (NIH P20 RR16462 from the Institutional Development Award Networks of Biomedical Research Excellence Program of the National Center for Research Resources) (B.A.B.). This work utilized the Cell and Molecular Biology Core(s) of the the Michigan Diabetes Research and Training Center funded by NIH5P60 DK20572 from NIDDK at the University of Michigan.

REFERENCES

1. **Alessi, D. R., L. R. Pearce, and J. M. Garcia-Martinez.** 2009. New insights into mTOR signaling: mTORC2 and beyond. Sci. Signal **2:**pe27.
2. **Avruch, J., K. Hara, Y. Lin, M. Liu, X. Long, S. Ortiz-Vega, and K. Yonezawa.** 2006. Insulin and amino-acid regulation of mTOR signaling and kinase activity through the Rheb GTPase. Oncogene **25:**6361–6372.
3. **Bai, X., D. Ma, A. Liu, X. Shen, Q. J. Wang, Y. Liu, and Y. Jiang.** 2007. Rheb activates mTOR by antagonizing its endogenous inhibitor, FKBP38. Science **318:**977–980.
4. **Bhaskar, P. T., and N. Hay.** 2007. The two TORCs and Akt. Dev. Cell **12:**487–502.
5. **Carriere, A., M. Cargnello, L. A. Julien, H. Gao, E. Bonneil, P. Thibault, and P. P. Roux.** 2008. Oncogenic MAPK signaling stimulates mTORC1 activity by promoting RSK-mediated raptor phosphorylation. Curr. Biol. **18:**1269–1277.
6. **Chen, J., X. F. Zheng, E. J. Brown, and S. L. Schreiber.** 1995. Identification of an 11-kDa FKBP12-rapamycin-binding domain within the 289-kDa FKBP12-rapamycin-associated protein and characterization of a critical serine residue. Proc. Natl. Acad. Sci. USA **92:**4947–4951.
7. **Cheng, S. W., L. G. Fryer, D. Carling, and P. R. Shepherd.** 2004. Thr2446 is a novel mammalian target of rapamycin (mTOR) phosphorylation site regulated by nutrient status. J. Biol. Chem. **279:**15719–15722.
8. **Chiang, G. G., and R. T. Abraham.** 2005. Phosphorylation of mammalian target of rapamycin (mTOR) at Ser-2448 is mediated by p70S6 kinase. J. Biol. Chem. **280:**25485–25490.
9. **Choi, J., J. Chen, S. L. Schreiber, and J. Clardy.** 1996. Structure of the FKBP12-rapamycin complex interacting with the binding domain of human FRAP. Science **273:**239–242.
10. **Choi, K. M., L. P. McMahon, and J. C. Lawrence, Jr.** 2003. Two motifs in the translational repressor PHAS-I required for efficient phosphorylation by mammalian target of rapamycin and for recognition by raptor. J. Biol. Chem. **278:**19667–19673.
11. **Dann, S. G., A. Selvaraj, and G. Thomas.** 2007. mTOR complex1-S6K1 signaling: at the crossroads of obesity, diabetes and cancer. Trends Mol. Med. **13:**252–259.

11a. **Daub, H., J. V. Olsen, M. Bairlein, F. Gnad, F. S. Oppermann, R. Korner, Z. Greff, G. Keri, O. Stemmann, and M. Mann.** 2008. Kinase-selective enrichment enables quantitative phosphoproteomics of the kinome across the cell cycle. Mol. Cell **31:**438–448.

12. **Dunlop, E. A., and A. R. Tee.** 2009. Mammalian target of rapamycin complex 1: signalling inputs, substrates and feedback mechanisms. Cell. Signal. **21:**827–835.
13. **Fang, Y., M. Vilella-Bach, R. Bachmann, A. Flanigan, and J. Chen.** 2001. Phosphatidic acid-mediated mitogenic activation of mTOR signaling. Science **294:**1942–1945.
14. **Fingar, D. C., and J. Blenis.** 2004. Target of rapamycin (TOR): an integrator of nutrient and growth factor signals and coordinator of cell growth and cell cycle progression. Oncogene **23:**3151–3171.
15. **Fingar, D. C., C. J. Richardson, A. R. Tee, L. Cheatham, C. Tsou, and J. Blenis.** 2004. mTOR controls cell cycle progression through its cell growth effectors S6K1 and 4E-BP1/eukaryotic translation initiation factor 4E. Mol. Cell. Biol. **24:**200–216.
16. **Fingar, D. C., S. Salama, C. Tsou, E. Harlow, and J. Blenis.** 2002. Mammalian cell size is controlled by mTOR and its downstream targets S6K1 and 4EBP1/eIF4E. Genes Dev. **16:**1472–1487.
17. **Fonseca, B. D., E. M. Smith, V. H. Lee, C. MacKintosh, and C. G. Proud.** 2007. PRAS40 is a target for mammalian target of rapamycin complex 1 and is required for signaling downstream of this complex. J. Biol. Chem. **282:**24514–24524.
18. **Frias, M. A., C. C. Thoreen, J. D. Jaffe, W. Schroder, T. Sculley, S. A. Carr, and D. M. Sabatini.** 2006. mSin1 is necessary for Akt/PKB phosphorylation, and its isoforms define three distinct mTORC2s. Curr. Biol. **16:**1865–1870.
19. **Garami, A., F. J. Zwartkruis, T. Nobukuni, M. Joaquin, M. Roccio, H. Stocker, S. C. Kozma, E. Hafen, J. L. Bos, and G. Thomas.** 2003. Insulin activation of Rheb, a mediator of mTOR/S6K/4E-BP signaling, is inhibited by TSC1 and 2. Mol. Cell **11:**1457–1466.

20. **Garcia-Martinez, J. M., and D. R. Alessi.** 2008. mTOR complex 2 (mTORC2) controls hydrophobic motif phosphorylation and activation of serum- and glucocorticoid-induced protein kinase 1 (SGK1). Biochem. J. **416:**375–385.
21. **Guertin, D. A., and D. M. Sabatini.** 2007. Defining the role of mTOR in cancer. Cancer Cell **12:**9–22.
22. **Guertin, D. A., and D. M. Sabatini.** 2009. The pharmacology of mTOR inhibition. Sci. Signal. **2:**pe24.
23. **Gwinn, D. M., D. B. Shackelford, D. F. Egan, M. M. Mihaylova, A. Mery, D. S. Vasquez, B. E. Turk, and R. J. Shaw.** 2008. AMPK phosphorylation of raptor mediates a metabolic checkpoint. Mol. Cell **30:**214–226.
24. **Hara, K., Y. Maruki, X. Long, K. Yoshino, N. Oshiro, S. Hidayat, C. Tokunaga, J. Avruch, and K. Yonezawa.** 2002. Raptor, a binding partner of target of rapamycin (TOR), mediates TOR action. Cell **110:**177–189.
25. **Holz, M. K., and J. Blenis.** 2005. Identification of S6K1 as a novel mTOR-phosphorylating kinase. J. Biol. Chem. **280:**26089–26093.
26. **Hresko, R. C., and M. Mueckler.** 2005. mTOR.RICTOR is the Ser473 kinase for Akt/protein kinase B in 3T3-L1 adipocytes. J. Biol. Chem. **280:**40406–40416.
27. **Huang, J., and B. D. Manning.** 2008. The TSC1-TSC2 complex: a molecular switchboard controlling cell growth. Biochem. J. **412:**179–190.
28. **Inoki, K., M. N. Corradetti, and K. L. Guan.** 2005. Dysregulation of the TSC-mTOR pathway in human disease. Nat. Genet. **37:**19–24.
29. **Inoki, K., Y. Li, T. Zhu, J. Wu, and K. L. Guan.** 2002. TSC2 is phosphorylated and inhibited by Akt and suppresses mTOR signalling. Nat. Cell Biol. **4:**648–657.
30. **Inoki, K., T. Zhu, and K. L. Guan.** 2003. TSC2 mediates cellular energy response to control cell growth and survival. Cell **115:**577–590.
31. **Jacinto, E.** 2008. What controls TOR? IUBMB Life **60:**483–496.
32. **Jacinto, E., R. Loewith, A. Schmidt, S. Lin, M. A. Ruegg, A. Hall, and M. N. Hall.** 2004. Mammalian TOR complex 2 controls the actin cytoskeleton and is rapamycin insensitive. Nat. Cell Biol. **6:**1122–1128.
33. **Kim, D. H., D. D. Sarbassov, S. M. Ali, J. E. King, R. R. Latek, H. Erdjument-Bromage, P. Tempst, and D. M. Sabatini.** 2002. mTOR interacts with raptor to form a nutrient-sensitive complex that signals to the cell growth machinery. Cell **110:**163–175.
34. **Kim, D. H., D. D. Sarbassov, S. M. Ali, R. R. Latek, K. V. Guntur, H. Erdjument-Bromage, P. Tempst, and D. M. Sabatini.** 2003. GβL, a positive regulator of the rapamycin-sensitive pathway required for the nutrient-sensitive interaction between raptor and mTOR. Mol. Cell **11:**895–904.
35. **Kim, E., P. Goraksha-Hicks, L. Li, T. P. Neufeld, and K. L. Guan.** 2008. Regulation of TORC1 by Rag GTPases in nutrient response. Nat. Cell Biol. **10:**935–945.
36. **Kwiatkowski, D. J., and B. D. Manning.** 2005. Tuberous sclerosis: a GAP at the crossroads of multiple signaling pathways. Hum. Mol. Genet. **14**(Spec. no. 2)**:**R251–R258.
37. **Kwiatkowski, D. J., H. Zhang, J. L. Bandura, K. M. Heiberger, M. Glogauer, N. el-Hashemite, and H. Onda.** 2002. A mouse model of TSC1 reveals sex-dependent lethality from liver hemangiomas, and up-regulation of p70S6 kinase activity in Tsc1 null cells. Hum. Mol. Genet. **11:**525–534.
38. **Long, X., Y. Lin, S. Ortiz-Vega, K. Yonezawa, and J. Avruch.** 2005. Rheb binds and regulates the mTOR kinase. Curr. Biol. **15:**702–713.
39. **Ma, L., Z. Chen, H. Erdjument-Bromage, P. Tempst, and P. P. Pandolfi.** 2005. Phosphorylation and functional inactivation of TSC2 by Erk implications for tuberous sclerosis and cancer pathogenesis. Cell **121:**179–193.
40. **Ma, X. M., and J. Blenis.** 2009. Molecular mechanisms of mTOR-mediated translational control. Nat. Rev. Mol. Cell Biol. **10:**307–318.
41. **MacDougald, O. A., P. Cornelius, R. Liu, and M. D. Lane.** 1995. Insulin regulates transcription of the CCAAT/enhancer binding protein (C/EBP) alpha, beta, and delta genes in fully-differentiated 3T3-L1 adipocytes. J. Biol. Chem. **270:**647–654.
42. **Manning, B. D., A. R. Tee, M. N. Logsdon, J. Blenis, and L. C. Cantley.** 2002. Identification of the tuberous sclerosis complex-2 tumor suppressor gene product tuberin as a target of the phosphoinositide 3-kinase/akt pathway. Mol. Cell **10:**151–162.
43. **Nave, B. T., M. Ouwens, D. J. Withers, D. R. Alessi, and P. R. Shepherd.** 1999. Mammalian target of rapamycin is a direct target for protein kinase B: identification of a convergence point for opposing effects of insulin and amino-acid deficiency on protein translation. Biochem. J. **344:**427–431.
44. **Nojima, H., C. Tokunaga, S. Eguchi, N. Oshiro, S. Hidayat, K. Yoshino, K. Hara, N. Tanaka, J. Avruch, and K. Yonezawa.** 2003. The mammalian target of rapamycin (mTOR) partner, raptor, binds the mTOR substrates p70 S6 kinase and 4E-BP1 through their TOR signaling (TOS) motif. J. Biol. Chem. **278:**15461–15464.
45. **Oshiro, N., R. Takahashi, K. Yoshino, K. Tanimura, A. Nakashima, S. Eguchi, T. Miyamoto, K. Hara, K. Takehana, J. Avruch, U. Kikkawa, and K. Yonezawa.** 2007. The proline-rich Akt substrate of 40 kDa (PRAS40) is a physiological substrate of mammalian target of rapamycin complex 1. J. Biol. Chem. **282:**20329–20339.
46. **Oshiro, N., K. Yoshino, S. Hidayat, C. Tokunaga, K. Hara, S. Eguchi, J. Avruch, and K. Yonezawa.** 2004. Dissociation of raptor from mTOR is a mechanism of rapamycin-induced inhibition of mTOR function. Genes Cells **9:**359–366.
47. **Pearce, L. R., X. Huang, J. Boudeau, R. Pawlowski, S. Wullschleger, M. Deak, A. F. Ibrahim, R. Gourlay, M. A. Magnuson, and D. R. Alessi.** 2007. Identification of Protor as a novel Rictor-binding component of mTOR complex-2. Biochem. J. **405:**513–522.
48. **Perry, J., and N. Kleckner.** 2003. The ATRs, ATMs, and TORs are giant HEAT repeat proteins. Cell **112:**151–155.
49. **Peterson, R. T., P. A. Beal, M. J. Comb, and S. L. Schreiber.** 2000. FKBP12-rapamycin-associated protein (FRAP) autophosphorylates at serine 2481 under translationally repressive conditions. J. Biol. Chem. **275:**7416–7423.
50. **Reiling, J. H., and D. M. Sabatini.** 2006. Stress and mTORture signaling. Oncogene **25:**6373–6383.
51. **Roux, P. P., B. A. Ballif, R. Anjum, S. P. Gygi, and J. Blenis.** 2004. Tumor-promoting phorbol esters and activated Ras inactivate the tuberous sclerosis tumor suppressor complex via p90 ribosomal S6 kinase. Proc. Natl. Acad. Sci. USA **101:**13489–13494.
52. **Sancak, Y., T. R. Peterson, Y. D. Shaul, R. A. Lindquist, C. C. Thoreen, L. Bar-Peled, and D. M. Sabatini.** 2008. The Rag GTPases bind raptor and mediate amino acid signaling to mTORC1. Science **320:**1496–1501.
53. **Sancak, Y., and D. M. Sabatini.** 2009. Rag proteins regulate amino-acid-induced mTORC1 signalling. Biochem. Soc. Trans. **37:**289–290.
54. **Sancak, Y., C. C. Thoreen, T. R. Peterson, R. A. Lindquist, S. A. Kang, E. Spooner, S. A. Carr, and D. M. Sabatini.** 2007. PRAS40 is an insulin-regulated inhibitor of the mTORC1 protein kinase. Mol. Cell **25:**903–915.
55. **Sarbassov, D. D., S. M. Ali, D. H. Kim, D. A. Guertin, R. R. Latek, H. Erdjument-Bromage, P. Tempst, and D. M. Sabatini.** 2004. Rictor, a novel binding partner of mTOR, defines a rapamycin-insensitive and raptor-independent pathway that regulates the cytoskeleton. Curr. Biol. **14:**1296–1302.
56. **Sarbassov, D. D., D. A. Guertin, S. M. Ali, and D. M. Sabatini.** 2005. Phosphorylation and regulation of Akt/PKB by the rictor-mTOR complex. Science **307:**1098–1101.
57. **Schalm, S. S., and J. Blenis.** 2002. Identification of a conserved motif required for mTOR signaling. Curr. Biol. **12:**632–639.
58. **Schalm, S. S., D. C. Fingar, D. M. Sabatini, and J. Blenis.** 2003. TOS motif-mediated raptor binding regulates 4E-BP1 multisite phosphorylation and function. Curr. Biol. **13:**797–806.
59. **Sekulic, A., C. C. Hudson, J. L. Homme, P. Yin, D. M. Otterness, L. M. Karnitz, and R. T. Abraham.** 2000. A direct linkage between the phosphoinositide 3-kinase-AKT signaling pathway and the mammalian target of rapamycin in mitogen-stimulated and transformed cells. Cancer Res. **60:**3504–3513.
60. **Stan, R., M. M. McLaughlin, R. Cafferkey, R. K. Johnson, M. Rosenberg, and G. P. Livi.** 1994. Interaction between FKBP12-rapamycin and TOR involves a conserved serine residue. J. Biol. Chem. **269:**32027–32030.
61. **Student, A. K., R. Y. Hsu, and M. D. Lane.** 1980. Induction of fatty acid synthetase synthesis in differentiating 3T3-L1 preadipocytes. J. Biol. Chem. **255:**4745–4750.
62. **Sun, Y., Y. Fang, M. S. Yoon, C. Zhang, M. Roccio, F. J. Zwartkruis, M. Armstrong, H. A. Brown, and J. Chen.** 2008. Phospholipase D1 is an effector of Rheb in the mTOR pathway. Proc. Natl. Acad. Sci. USA **105:**8286–8291.
63. **Tee, A. R., R. Anjum, and J. Blenis.** 2003. Inactivation of the tuberous sclerosis complex-1 and -2 gene products occurs by phosphoinositide 3-kinase/Akt-dependent and -independent phosphorylation of tuberin. J. Biol. Chem. **278:**37288–37296.
64. **Tee, A. R., D. C. Fingar, B. D. Manning, D. J. Kwiatkowski, L. C. Cantley, and J. Blenis.** 2002. Tuberous sclerosis complex-1 and -2 gene products function together to inhibit mammalian target of rapamycin (mTOR)-mediated downstream signaling. Proc. Natl. Acad. Sci. USA **99:**13571–13576.
65. **Tee, A. R., B. D. Manning, P. P. Roux, L. C. Cantley, and J. Blenis.** 2003. Tuberous sclerosis complex gene products, Tuberin and Hamartin, control mTOR signaling by acting as a GTPase-activating protein complex toward Rheb. Curr. Biol. **13:**1259–1268.
66. **Thedieck, K., P. Polak, M. L. Kim, K. D. Molle, A. Cohen, P. Jeno, C. Arrieumerlou, and M. N. Hall.** 2007. PRAS40 and PRR5-like protein are new mTOR interactors that regulate apoptosis. PLoS ONE **2:**e1217.
67. **van der Haar, E., S. I. Lee, S. Bandhakavi, T. J. Griffin, and D. H. Kim.** 2007. Insulin signaling to mTOR mediated by the AKT/PKB substrate PRAS40. Nat. Cell Biol. **9:**316–323.
68. **Wang, L., T. E. Harris, and J. C. Lawrence, Jr.** 2008. Regulation of proline-rich Akt substrate of 40 kDa (PRAS40) function by mammalian target of rapamycin complex 1 (mTORC1)-mediated phosphorylation. J. Biol. Chem. **283:**15619–15627.
69. **Wang, L., T. E. Harris, R. A. Roth, and J. C. Lawrence, Jr.** 2007. PRAS40 regulates mTORC1 kinase activity by functioning as a direct inhibitor of substrate binding. J. Biol. Chem. **282:**20036–20044.
70. **Wang, L., J. C. Lawrence, T. W. Sturgill, and T. E. Harris.** 2009. Mammalian target of rapamycin complex 1 (mTORC1) activity is associated with phosphorylation of raptor by mTOR. J. Biol. Chem. **284:**14693–14697.
71. **Wang, L., C. J. Rhodes, and J. C. Lawrence, Jr.** 2006. Activation of mammalian target of rapamycin (mTOR) by insulin is associated with stimulation of 4EBP1 binding to dimeric mTOR complex 1. J. Biol. Chem. **281:**24293–24303.

72. **Wang, X., B. D. Fonseca, H. Tang, R. Liu, A. Elia, M. J. Clemens, U. A. Bommer, and C. G. Proud.** 2008. Re-evaluating the roles of proposed modulators of mammalian target of rapamycin complex 1 (mTORC1) signaling. J. Biol. Chem. **283:**30482–30492.
73. **Woo, S. Y., D. H. Kim, C. B. Jun, Y. M. Kim, E. V. Haar, S. I. Lee, J. W. Hegg, S. Bandhakavi, and T. J. Griffin.** 2007. PRR5, a novel component of mTOR complex 2, regulates platelet-derived growth factor receptor beta expression and signaling. J. Biol. Chem. **282:**25604–25612.
74. **Wullschleger, S., R. Loewith, and M. N. Hall.** 2006. TOR signaling in growth and metabolism. Cell **124:**471–484.
75. **Wullschleger, S., R. Loewith, W. Oppliger, and M. N. Hall.** 2005. Molecular organization of target of rapamycin complex 2. J. Biol. Chem. **280:**30697–30704.
76. **Yang, Q., K. Inoki, T. Ikenoue, and K. L. Guan.** 2006. Identification of Sin1 as an essential TORC2 component required for complex formation and kinase activity. Genes Dev. **20:**2820–2832.